Inorganic Chemistry
Article

Inorg. Chem. **2011**, *50*, 883–899 **883**
DOI: 10.1021/ic101475x

Complex Formation in Aqueous Solution and in the Solid State of the Potent Insulin-Enhancing $V^{IV}O^{2+}$ Compounds Formed by Picolinate and Quinolinate Derivatives

Elzbieta Lodyga-Chruscinska,[†] Giovanni Micera,[‡] and Eugenio Garribba*[,‡]

[†]*Institute of General Food Chemistry, Technical University of Lodz, ul. Stefanowskiego 4/10, PL-90924, Lodz, Poland, and* [‡]*Dipartimento di Chimica e Centro Interdisciplinare per lo Sviluppo della Ricerca Biotecnologica e per lo Studio della Biodiversità della Sardegna, Università di Sassari, Via Vienna 2, I-07100 Sassari, Italy*

Received July 23, 2010

The complexation of $V^{IV}O^{2+}$ ion with 10 picolinate and quinolinate derivatives, provided with the donor set (N, COO^-), was studied in aqueous solution and in the solid state through the combined application of potentiometric (pH-titrations), spectroscopic (EPR, UV/vis and IR spectroscopy), and computational (density functional theory (DFT) calculations) methods. Such derivatives, that form potent insulin-enhancing $V^{IV}O^{2+}$ compounds, are picolinic (picH), 6-methylpicolinic (6-mepicH), 3-methylpicolinic (3-mepicH), 5-butylpicolinic or fusaric (fusarH), 6-methyl-2,3-pyridindicarboxylic (6-me-2,3-pdcH_2), 2-pyridylacetic (2-pyacH), 2-quinolinecarboxylic or quinaldic (quinH), 4-hydroxyquinoline-2-carboxylic or kynurenic (kynurH), 1-isoquinolinecarboxylic (1-iqcH) and 3-isoquinolinecarboxylic (3-iqcH) acid. On the basis of the potentiometric, spectroscopic, and DFT results, they were divided into the classes A, B, and C. The ligands belonging to class A (3-mepicH, 1-iqcH, 2-pyacH) form square pyramidal complexes in aqueous solution and in the solid state, and those belonging to class B (picH, fusarH, 3-iqcH) form *cis*-octahedral species, in which the two ligands adopt an (equatorial-equatorial) and an (equatorial-axial) arrangement and one water molecule occupies an equatorial site in *cis* position with respect to the V═O bond. Class C ligands (6-mepicH, 6-me-2,3-pdcH_2, quinH, kynurH) yield bis chelated species, that in water are in equilibrium between the square pyramidal and *trans*-octahedral form, where both the ligand molecules adopt an (equatorial-equatorial) arrangement and one water is in *trans* position with respect to the V═O group. The *trans*-octahedral compounds are characterized by an anomalous electron paramagnetic resonance (EPR) response, with A_z value being reduced by about 10% with respect to the prediction of the "additivity rule". DFT methods allow to calculate the structure, ^{51}V hyperfine coupling constant (A_z), the stretching frequency of V═O bond ($\nu_{V=O}$), the relative stability in aqueous solution, and the electronic structure and molecular orbital composition of bis chelated complexes. The results were used to explain the biotransformation of these potent insulin-enhancing compounds in blood serum.

Introduction

Vanadium plays a number of functions in the biological systems.[1] It is commonly accepted that vanadium plays an essential role in the higher animals, even if its biochemical functions still remain unclear.[2] In human organism, it elicits a number of physiological responses, for example, the inhibition of phosphate-metabolizing enzymes, such as phosphatases, ribonuclease, and ATPases.[3]

One of the most important applications of vanadium compounds is the potential use in the therapy of patients suffering from type II diabetes mellitus (DM),[1,4−6] which affects worldwide 150 million people according to the estimates of World Health Organization.[1b] Since type II diabetes goes along with an increasing lack of response to insulin,

*To whom correspondence should be addressed. E-mail: garribba@uniss.it.

(1) (a) Crans, D. C.; Smee, J. J.; Gaidamauskas, E.; Yang, L. *Chem. Rev.* **2004**, *104*, 849–902. (b) Rehder, D. *Bioinorganic Vanadium Chemistry*; Wiley: Chichester, 2008.

(2) (a) Nielsen, F. H. In *Metal Ions in Biological Systems*; Sigel, A., Sigel, H., Eds.; Marcel Dekker: New York, 1995; Vol. *31*, pp 543−573. (b) Nielsen, F. H. In *Vanadium Compounds: Chemistry, Biochemistry, and Therapeutic Applications*; Tracey, A. S., Crans, D. C., Eds.; ACS symposium series 711; American Chemical Society: Washington, DC, 1998; pp 297−315.

(3) Stankiewicz, P. J.; Tracey, A. S.; Crans, D. C. In *Metal Ions in Biological Systems*; Sigel, A., Sigel, H., Eds.; Marcel Dekker: New York, 1995; Vol. *31*, pp 287−324.

(4) (a) Thompson, K. H.; McNeill, J. H.; Orvig, C. *Chem. Rev.* **1999**, *99*, 2561–2571, and references therein. (b) Thompson, K. H.; Orvig, C. *Dalton Trans.* **2000**, 2885–2892. (c) Thompson, K. H.; Orvig, C. *Coord. Chem. Rev.* **2001**, *219−221*, 1033–1053, and references therein.

(5) Shechter, Y.; Goldwaser, I.; Mironchik, M.; Fridkin, M.; Gefel, D. *Coord. Chem. Rev.* **2003**, *237*, 3–11.

(6) (a) Sakurai, H.; Kojima, Y.; Yoshikawa, Y.; Kawabe, K.; Yasui, H. *Coord. Chem. Rev.* **2002**, *226*, 187–198. (b) Kawabe, K.; Yoshikawa, Y.; Adachi, Y.; Sakurai, H. *Life Sci.* **2006**, *78*, 2860–2866.

Published on Web 01/12/2011

insulin injections can ultimately become ineffective and alternative methods of treatment are desirable. About 30 years ago, an in vitro study on the insulin-enhancing action of vanadate was published, revealing the vanadate-stimulated uptake and degradation of glucose by adipocytes (fat cells), the stimulation of glycogenesis in the liver, and the inhibition of hepatic gluconeogenesis;[7] these effects were related to the reduction of vanadate(V) to vanadyl $V^{IV}O^{2+}$, and the action of $V^{IV}O^{2+}$ ion in the inhibition of a cellular phosphatase.[8] Vanadium species have the advantage over insulin of a possible oral administration.

After the initial use of vanadium(IV) and vanadium(V) inorganic salts, not easily applicable as antidiabetic drugs because of their toxicity and the very low absorption rate, several peroxovanadium(V) complexes with (N,N), (N,O), and (O,O) ligands[9] and particularly neutral vanadyl species (VOL_2, where the bidentate monoanionic ligand L is also called organic *carrier*) were tested.[4−6] Most of these compounds stimulate glucose intake into cells, inhibit free fatty acid (FFA) release and gluconeogenesis, stimulate lypogenesis, and reduce or restore blood glucose level.

$V^{IV}O^{2+}$ complexes with [VOL_2] stoichiometry are more effective in lowering the glucose concentration in blood serum than $VOSO_4$ and are well tolerated in all animal models of diabetes. The insulin-enhancing properties of compounds with coordination mode $VO(O_4)$,[10,11] $VO(N_2O_2)$,[6,12,13] $VO(N_2S_2)$,[10,14] $VO(O_2S_2)$,[15] $VO(N_4)$,[16] and $VO(S_4)$[17] have been examined. Generally, (N, O) ligation is more efficient than (O, O) or (O/N, S) coordination, irrespective of the vanadium oxidation state.[18]

$V^{IV}O^{2+}$ compounds with $VO(N_2O_2)$ coordination are very promising in the treatment of insulin dependent diabetes mellitus.[19,20] In 1995 [$VO(picolinato)_2(H_2O)$] was found to be a strong inhibitor of fatty acid mobilization and effective in the treatment of rats affected by diabetes induced with streptozotocin (STZ).[12] Subsequently, [VO(6-methylpicolinato)$_2$] was discovered to exhibit better in vitro insulin-enhancing and in vivo hypoglycemic effect in STZ-rats than parent $V^{IV}O^{2+}$-picolinate species;[13,21] in particular, it shows long-acting character and low toxicity and is very effective in the treatment of insulin-dependent diabetes mellitus (IDDM) as well as not insulin-dependent diabetes mellitus (NIDDM) when studied in vitro and in vivo experiments.[22] Subsequently, several $V^{IV}O^{2+}$ complexes formed by picolinate derivatives were tested, such as [VO(2-quinolinecarboxylato)$_2$],[19] [VO(3-methylpicolinato)$_2$],[23] [VO(5-iodopicolinato)$_2$],[24] *trans*-[$VO(6\text{-ethylpicolinato})_2(H_2O)$],[25] *cis*-[$VO(3\text{-hydroxypicolinato})_2(H_2O)$],[26] *cis*-[$VO(5\text{-carbomethoxypicolinato})_2(H_2O)$],[27] and the bis chelated *cis*-octahedral species formed by 2,5-dipicolinic acid and its monoesters.[28] The results suggested that not only the electronic character of the substituent but also its position on the pyridine ring can alter the biological activity of the complex; in particular, the introduction of an electron-withdrawing halogen atom or an electron-donating alkyl group at the fifth or third position of the aromatic ring results in an insulin-enhancing activity stronger than lead complex *cis*-[$VO(picolinato)_2(H_2O)$] or $VOSO_4$.

Therefore, in the design of new active $V^{IV}O^{2+}$ compounds, the relation between the physio-chemical properties, in vitro insulin-enhancing action, and in vivo hypoglycemic activity must be examined. In particular, it seems to be crucial to know the biotransformation of an insulin-enhancing drug in blood serum around the physiological pH; for example, the existence of mixed species between [VO(maltolato)$_2$] and transferrin or albumin, proposed by Willsky et al.[29] and Orvig and co-workers,[30] could be so important in the transport of the drug to be considered the pharmacologically active species. It has been demonstrated recently that, if the geometry of the insulin-enhancing compound in aqueous solution is *cis*-octahedral (for example, with 1,2-dimethyl-3-hydroxy-4(1*H*)-pyridinonate),[31] mixed complexes with transferrin and albumin with stoichiometry *cis*-VO(*carrier*)$_2$-(hTf) and *cis*-VO(*carrier*)$_2$(HSA) (hTf and HSA are human

(7) Tolman, E. L.; Barris, E.; Burns, M.; Pansini, A.; Partridge, R. *Life Sci*. **1979**, *25*, 1159–1164.
(8) Shechter, Y.; Karlish, S. J. D. *Nature* **1980**, *286*, 556–558.
(9) (a) Posner, B. I.; Faure, R.; Burgess, J. W.; Bevan, A. P.; Lachance, D.; Zhang-Sun, G.; Fantus, I. G.; Ng, J. B.; Hall, D. A.; Soo Lum, B.; Shaver, A. *J. Biol. Chem*. **1994**, *269*, 4596–4606. (b) Posner, B. I.; Yang, C. R.; Shaver, A. In *Vanadium Compounds: Chemistry, Biochemistry, and Therapeutic Applications*; Tracey, A. S., Crans, D. C., Eds.; ACS symposium series 711; American Chemical Society: Washington, DC, 1998; pp 316−328.
(10) Sakurai, H.; Tsuchiya, K.; Nukatsuka, M.; Kawada, J.; Ishikawa, S.; Komatsu, M. *J. Clin. Biochem. Nutr*. **1990**, *8*, 193–200.
(11) (a) Reul, B. A.; Amin, S. S.; Buchet, J. P.; Ongemba, L. N.; Crans, D. C.; Brichard, S. M. *Br. J. Pharmacol*. **1999**, *126*, 467–477. (b) Amin, S. S.; Cryer, K.; Zhang, B.; Dutta, S. K.; Eaton, S. S.; Anderson, O. P.; Miller, S. M.; Reul, B. A.; Brichard, S. M.; Crans, D. C. *Inorg. Chem*. **2000**, *39*, 406–416.
(12) Sakurai, H.; Fujii, K.; Watanabe, H.; Tamura, H. *Biochem. Biophys. Res. Commun*. **1995**, *214*, 1095–1101.
(13) Fujimoto, S.; Fujii, K.; Yasui, H.; Matsushita, R.; Takada, J.; Sakurai, H. *J. Clin. Biochem. Nutr*. **1997**, *23*, 113–129.
(14) Cam, M. C.; Cros, G. H.; Serrano, J. J.; Lazaro, R.; McNeill, J. H. *Diabetes Res. Clin. Pract*. **1993**, *20*, 111–121.
(15) (a) Sakurai, H.; Sano, H.; Takino, T.; Yasui, H. *Chem. Lett*. **1999**, 913–914. (b) Sakurai, H.; Sano, H.; Takino, T.; Yasui, H. *J. Inorg. Biochem*. **2000**, *80*, 99–105.
(16) Woo, L. C.; Yuen, V. G.; Thompson, K. H.; McNeill, J. H.; Orvig, C. *J. Inorg. Biochem*. **1999**, *76*, 251–257.
(17) (a) Watanabe, H.; Nakai, M.; Komazawa, K.; Sakurai, H. *J. Med. Chem*. **1994**, *37*, 876–877. (b) Sakurai, H.; Watanabe, H.; Tamura, H.; Yasui, H.; Matsushita, R.; Takada, J. *Inorg. Chim. Acta* **1998**, *283*, 175–183.
(18) Rehder, D.; Costa Pessoa, J.; Geraldes, C. F. G. C.; Castro, M. M. C. A.; Kabanos, T.; Kiss, T.; Meier, B.; Micera, G.; Pettersson, L.; Rangel, M.; Salifoglou, A.; Turel, I.; Wang, D. *J. Biol. Inorg. Chem*. **2002**, *7*, 384–396.
(19) Sakurai, H.; Fujii, K.; Fujimoto, S.; Fujisawa, Y.; Takechi, K.; Yasui, H. In *Vanadium Compounds: Chemistry, Biochemistry, and Therapeutic Applications*; Tracey, A. S., Crans, D. C., Eds.; ACS symposium series 711; American Chemical Society: Washington, DC, 1998; pp 344−352.
(20) Sakurai, H. In *Vanadium: the Versatile Metal*; Kustin, K., Costa Pessoa, J., Crans, D. C., Eds.; ACS Symposium Series 974; American Chemical Society: Washington, DC, 2007; pp 110−120.
(21) Fujisawa, Y.; Sakurai, H. *Chem. Pharm. Bull*. **1999**, *47*, 1668–1670.
(22) Sakurai, H.; Fujisawa, Y.; Fujimoto, S.; Yasui, H.; Takino, T. *J. Trace Elem. Exp. Med*. **1999**, *12*, 393–401.
(23) Sakurai, H.; Tamura, A.; Takino, T.; Ozutsumi, K.; Kawabe, K.; Kojima, Y. *Inorg. React. Mech*. **2000**, *2*, 69–77.
(24) Takino, T.; Yasui, H.; Yoshitake, A.; Hamajima, Y.; Matsushita, R.; Takada, J.; Sakurai, H. *J. Biol. Inorg. Chem*. **2001**, *6*, 133–142.
(25) Sasagawa, T.; Yoshikawa, Y.; Kawabe, K.; Sakurai, H.; Kojima, Y. *J. Inorg. Biochem*. **2002**, *88*, 108–112.
(26) Yano, S.; Nakai, M.; Sekiguchi, F.; Obata, M.; Kato, M.; Shiro, M.; Kinoshita, I.; Mikuria, M.; Sakurai, H.; Orvig, C. *Chem. Lett*. **2002**, 916–917.
(27) Gätjens, J.; Meier, B.; Kiss, T.; Nagy, E. M.; Buglyó, P.; Sakurai, H.; Kawabe, K.; Rehder, D. *Chem.—Eur. J*. **2003**, *9*, 4924–4935.
(28) Gätjens, J.; Meier, B.; Adachi, Y.; Sakurai, H.; Rehder, D. *Eur. J. Inorg. Chem*. **2006**, 3575–3585.
(29) Willsky, G. R.; Goldfine, A. B.; Kostyniak, P. J.; McNeill, J. H.; Yang, L. Q.; Khan, H. R.; Crans, D. C. *J. Inorg. Biochem*. **2001**, *85*, 33–42.
(30) Liboiron, B. D.; Thompson, K. H.; Hanson, G. R.; Lam, E.; Aebischer, N.; Orvig, C. *J. Am. Chem. Soc*. **2005**, *127*, 5104–5115.
(31) The nomenclature *cis*-octahedral refers to the hexa-coordinated complexes in which the two ligands adopt an (equatorial-equatorial) and an (equatorial-axial) arrangement and one water molecule occupies an equatorial site in *cis* position with respect to the V=O bond; *trans*-octahedral are the hexa-coordinated complexes in which both the ligands adopt an (equatorial-equatorial) arrangement and one water molecule is in *trans* position with respect to the V=O group.

Scheme 1. Class A, B, and C Ligands and $V^{IV}O^{2+}$ Complexes Formed: (a) Penta-Coordinated Square Pyramidal; (b) Hexa-Coordinated *cis*-Octahedral, and (c) Hexa-Coordinated *trans*-Octahedral Species[a]

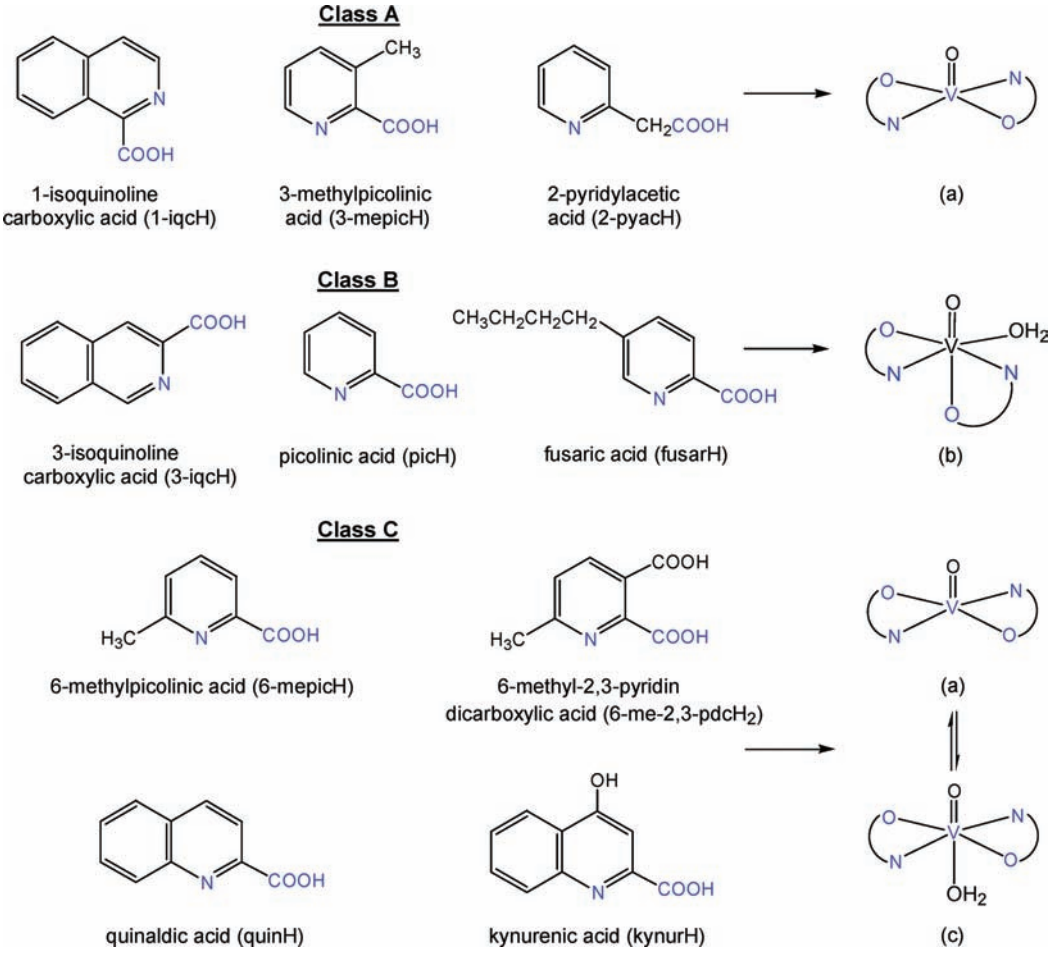

[a] For class C ligands, the equilibrium between the square pyramidal and *trans*-octahedral form is shown.

serum transferrin and human serum albumin) can be formed; in such complexes an imidazole nitrogen of a histidine residue belonging to hTf or HSA polypeptide chain replaces H_2O ligand in the equatorial position. On the contrary, if the *carrier* is weak (6-methylpicolinate) or forms square pyramidal species (acetylacetonate) the formation of ternary species is not favored, and $(VO)_2$hTf in the first case and $(VO)_2$hTF and [VO(*carrier*)$_2$] in the second one are the main species in the aqueous solution around pH 7.4.[32]

Since the relation between the structure in the solid state and in water and the insulin-enhancing activity appears certain, in this work the interaction of $V^{IV}O^{2+}$ ion with 10 derivatives of picolinic acid, provided with the donor set (N, COO^-), was studied through the combined application of potentiometric (pH-titrations), spectroscopic (EPR, UV/vis, and IR spectroscopy) and computational (density functional theory (DFT) calculations) methods.

According to the chemical and spectroscopic behavior, they were divided into the three classes A, B, and C (Scheme 1). The ligands belonging to class A (3-mepicH, 1-iqcH, 2-pyacH) form square pyramidal complexes, whereas those belonging to class B (picH, fusarH, 3-iqcH) form *cis*-octahedral species.[31] Class C ligands (6-mepicH, 6-me-2,3-pdcH$_2$, quinH, kynurH) yield bis chelated species that in water undergo an equilibrium between the square pyramidal and *trans*-octahedral form.

Experimental and Computational Section

Chemicals. Water was deionized prior to use through the purification system Millipore Milli-Q Academic. All the ligands were of the highest grade available and were used as received. VO^{2+} solutions were prepared from $VOSO_4 \cdot 3H_2O$ following literature methods.[33]

Potentiometric Measurements. The stability constants of proton and $V^{IV}O^{2+}$ complexes were determined by pH-potentiometric titrations on 2.0 mL of sample. The ligand to metal molar ratio was 1:1, 2:1, 4:1, and 10:1, and the $V^{IV}O^{2+}$ concentration 0.001, 0.002, and 0.004 M. Titrations were performed from pH 2.0 until precipitation or very extensive hydrolysis by adding carbonate-free NaOH of known concentration (ca. 0.1 M).[34] Because of the low solubility, the values regarding kynurenic acid and its $V^{IV}O^{2+}$ complexes were measured in a mixture H_2O/DMSO 50:50 v/v.

Measurements were carried out at 25.0 ± 0.1 °C and at a constant ionic strength of 0.2 M (KCl) with a MOLSPIN pH-meter equipped with a digitally operated syringe (the Molspin DSI 0.250 mL) controlled by a computer. The values of pH were measured with a Russel CMAWL/S7 semimicro combined electrode, calibrated for hydrogen ion concentration by the

(32) Sanna, D.; Micera, G.; Garribba, E. *Inorg. Chem.* **2010**, *49*, 174–187.
(33) Nagypál, I.; Fábián, I. *Inorg. Chim. Acta* **1982**, *61*, 109–113.
(34) Gran, G. *Acta Chem. Scand.* **1950**, *4*, 559–577.

Table 1. Protonation Constants (log β) of the Ligands at 25.0 ± 0.1 °C and I = 0.20 M (KCl)[a]

class	ligand	log β_1[b]	log β_2[c]	log β_3[d]	ref.
A	3-mepicH	5.18(1)	6.38(2)		this work
A	1-iqcH	5.04(1)	7.18(1)		this work
A	2-pyacH	5.71(1)	8.47(1)		this work
B	picH	5.19	6.19		50
B	fusarH	5.78(1)	7.60(1)		this work
B	3-iqcH	5.63(1)	7.56(1)		this work
C	6-mepicH	5.82	6.82		51
C	6-me-2,3-pdcH$_2$	5.44(1)	8.26(1)	10.66(1)	this work
C	quinH	4.89(1)	6.94(1)		this work
C	kynurH[e]	10.72(1)	12.22(1)		this work

[a] The uncertainties (σ values) are given between parentheses. [b] Attributable to the protonation of pyridine-N or quinoline-N. [c] Attributable to the protonation of COO^- group. [d] Attributable to the protonation of the second COO^- group. [e] Values measured in a mixture H_2O/DMSO 50:50 v/v.

method of Irving et al.[35] Purified argon was bubbled through the samples to ensure the absence of oxygen. The number of experimental points was 100−150 for each titration curve, and the reproducibility of the points included in the evaluation was within 0.005 pH unit in the whole pH range measured.

The stability of the complexes, reported as the logarithm of the overall formation constant $\beta_{pqr} = [(VO)_pL_qH_r]/[VO]^p[L]^q[H]^r$, where VO stands for $V^{IV}O^{2+}$ ion, L is the deprotonated form of the ligand, and H is the proton, were calculated with the aid of the SUPERQUAD programs.[36] Standard deviations were calculated by assuming random errors. The conventional notation has been used: negative indices for protons indicate either the dissociation of groups which do not deprotonate in the absence of $V^{IV}O^{2+}$ coordination, or hydroxido ligands. Hydroxido complexes of $V^{IV}O^{2+}$ were taken into account and the following species were assumed: $[VO(OH)]^+$ (log $\beta_{10-1} = -5.94$), $[(VO)_2(OH)_2]^{2+}$ (log $\beta_{20-2} = -6.95$), with stability constants calculated from the data of Henry et al.[37] and corrected for the different ionic strength by use of the Davies equation,[38] $[VO(OH)_3]^-$ (log $\beta_{10-3} = -18.0$) and $[(VO)_2(OH)_5]^-$ (log $\beta_{20-5} = -22.0$).[39] The uncertainty (σ values) of the stability constants are given in parentheses in Tables 1 and 2.

Synthesis of the Solid-State Complexes. $[VO(6\text{-mepic})_2]$ and *cis*-$[VO(pic)_2(H_2O)]$ were obtained by reaction at room temperature of an aqueous solution of $VOSO_4 \cdot 3H_2O$ (2×10^{-2} M) with the ligand (4×10^{-2} M) at pH 5. $[VO(1\text{-iqc})_2]$, $[VO(3\text{-mepic})_2]$, $[VO(2\text{-pyac})_2]$, *cis*-$[VO(3\text{-iqc})_2(H_2O)]$, *cis*-$[VO(fusar)_2(H_2O)]$, *trans*-$[VO(quin)_2(H_2O)]$ and *trans*-$[VO(kynur)_2(H_2O)]$, were synthesized by reaction at 40 °C, dissolving 0.04 mmol of $VOSO_4 \cdot 3H_2O$ and 0.08 mmol of the ligand in 50 mL of water at pH 3−3.5 under stirring. The polycrystalline samples were filtered off, washed with water, and dried at room temperature. $[VO(6\text{-mepic})_2]$. Anal. Calcd for $C_{14}H_{12}N_2O_5V$ (339.20): C, 49.57; H, 3.57; N, 8.26; H_2O, 0.0; V_2O_5, 26.8. Found: C, 49.55; H, 3.68; N, 8.16; H_2O, 0.0; V_2O_5, 26.0. *cis*-$[VO(pic)_2(H_2O)]$. Anal. Calcd for $C_{12}H_{10}N_2O_6V$ (329.16): C, 43.79; H, 3.06; N, 8.51; H_2O, 5.5; V_2O_5, 27.6. Found: C, 43.64; H, 3.19; N, 8.38; H_2O, 6.2; V_2O_5, 26.8. $[VO(1\text{-iqc})_2]$. Anal. Calcd for $C_{20}H_{12}N_2O_5V$ (411.27): C, 58.41; H, 2.94; N, 6.81; H_2O, 0.0; V_2O_5, 22.1. Found: C, 58.53; H, 3.09; N, 6.73; H_2O, 0.0; V_2O_5, 21.5. $[VO(3\text{-mepic})_2]$. Anal. Calcd for $C_{14}H_{12}N_2O_5V$ (339.20): C, 49.57; H, 3.57; N, 8.26; H_2O, 0.0; V_2O_5, 26.8. Found: C, 49.71; H, 3.48; N, 8.34; H_2O, 0.0; V_2O_5, 27.0. $[VO(2\text{-pyac})_2]$. Anal. Calcd for $C_{14}H_{12}N_2O_5V$ (339.20): C, 49.57; H, 3.57; N, 8.26; H_2O, 0.0; V_2O_5, 26.8. Found: C, 49.45; H, 3.58; N, 8.39; H_2O, 0.0; V_2O_5, 26.2. *cis*-$[VO(3\text{-iqc})_2(H_2O)]$. Anal. Calcd for $C_{20}H_{14}N_2O_6V$ (429.28): C, 55.96; H, 3.29; N, 6.53; H_2O, 4.2; V_2O_5, 21.2. Found: C, 55.99; H, 3.36; N, 6.47; H_2O, 4.0; V_2O_5, 20.8. *cis*-$[VO(fusar)_2(H_2O)]$. Anal. Calcd for $C_{20}H_{26}N_2O_5V$ (425.38): C, 56.47; H, 6.16; N, 6.59; H_2O, 4.2; V_2O_5, 21.4. Found: C, 56.61; H, 6.24; N, 6.47; H_2O, 4.0; V_2O_5, 21.0. *trans*-$[VO(quin)_2(H_2O)]$. Anal. Calcd for $C_{20}H_{14}N_2O_6V$ (429.28): C, 55.96; H, 3.29; N, 6.53; H_2O, 4.2; V_2O_5, 21.2. Found: C, 55.89; H, 3.15; N, 6.40; H_2O, 4.4; V_2O_5, 20.6. *trans*-$[VO(kynur)_2(H_2O)]$. Anal. Calcd for $C_{20}H_{14}N_2O_8V$ (461.28): C, 52.08; H, 3.06; N, 6.07; H_2O, 3.9; V_2O_5, 19.7. Found: C, 51.91; H, 2.99; N, 6.14; H_2O, 4.0; V_2O_5, 19.8.

Spectroscopic and Analytical Measurements. Anisotropic electron paramagnetic resonance (EPR) spectra were recorded on aqueous solutions with an X-band (9.15 GHz) Varian E-9 spectrometer at 100 K. As usual for low temperature measurements, a few drops of dimethylsulfoxide (DMSO) were added to the samples to ensure good glass formation. All operations were performed under a purified argon atmosphere to avoid oxidation of $V^{IV}O^{2+}$ ion. EPR spectra were simulated with the computer program Bruker WinEPR SimFonia.[40] Electronic absorption spectra on the aqueous solution were recorded with a Jasco Uvidec 610 spectrophotometer in the same concentration range as used for potentiometry and on the solid samples with a Beckman Acta MIV spectrophotometer employing the diffuse reflectance technique with $BaSO_4$ as reference sample. Infrared spectra (4000−600 cm^{-1}) were obtained with a Jasco FT/IR-480Plus spectrometer using KBr disks. Thermogravimetric data were obtained with a Perkin-Elmer TGS-2 apparatus under a nitrogen flow. Elemental analysis (C, H, N) was carried out with a Perkin-Elmer 240 B elemental analyzer.

DFT Calculations. All the calculations presented in this paper were performed with DFT methods,[41] and Gaussian 03 (revision C.02) software.[42] The hybrid exchange-correlation B3P86[43,44] and B3LYP,[43,45] the generalized gradient approximation PBE,[46] and the half-and-half BHandHLYP functional, as incorporated in the Gaussian 03, were used. The performance of

(35) Irving, H.; Miles, M. G.; Pettit, L. D. *Anal. Chim. Acta* **1967**, *38*, 475–488.
(36) Gans, P.; Vacca, A.; Sabatini, A. *J. Chem. Soc., Dalton Trans.* **1985**, 1195–1200.
(37) Henry, R. P.; Mitchell, P. C. H.; Prue, J. E. *J. Chem. Soc., Dalton Trans.* **1973**, 1156–1159.
(38) Davies, C. W. *J. Chem. Soc.* **1938**, 2093–2098.
(39) (a) Komura, A.; Hayashi, M.; Imanaga, H. *Bull. Chem. Soc. Jpn.* **1977**, *50*, 2927–2931. (b) Vilas Boas, L. F.; Costa Pessoa, J. In *Comprehensive Coordination Chemistry*; Wilkinson, G., Gillard, R. D., McCleverty, J. A., Eds.; Pergamon Press: Oxford, 1987; Vol. *3*, pp 453−583.
(40) *WINEPR SimFonia*, version 1.25; Bruker Analytische Messtechnik GmbH: Karlsruhe, Germany, 1996.
(41) Parr, R. G.; Yang, W. *Density-Functional Theory of Atoms and Molecules*; Oxford University Press: Oxford, 1989.
(42) Frisch, M. J.; Trucks, G. W.; Schlegel, H. B.; Scuseria, G. E.; Robb, M. A.; Cheeseman, J. R.; Montgomery, J. A., Jr.; Vreven, T.; Kudin, K. N.; Burant, J. C.; Millam, J. M.; Iyengar, S. S.; Tomasi, J.; Barone, V.; Mennucci, B.; Cossi, M.; Scalmani, G.; Rega, N.; Petersson, G. A.; Nakatsuji, H.; Hada, M.; Ehara, M.; Toyota, K.; Fukuda, R.; Hasegawa, J.; Ishida, M.; Nakajima, T.; Honda, Y.; Kitao, O.; Nakai, H.; Klene, M.; Li, X.; Knox, J. E.; Hratchian, H. P.; Cross, J. B.; Adamo, C.; Jaramillo, J.; Gomperts, R.; Stratmann, R. E.; Yazyev, O.; Austin, A. J.; Cammi, R.; Pomelli, C.; Ochterski, J. W.; Ayala, P. Y.; Morokuma, K.; Voth, G. A.; Salvador, P.; Dannenberg, J. J.; Zakrzewski, V. G.; Dapprich, S.; Daniels, A. D.; Strain, M. C.; Farkas, O.; Malick, D. K.; Rabuck, A. D.; Raghavachari, K.; Foresman, J. B.; Ortiz, J. V.; Cui, Q.; Baboul, A. G.; Clifford, S.; Cioslowski, J.; Stefanov, B. B.; Liu, G.; Liashenko, A.; Piskorz, P.; Komaromi, I.; Martin, R. L.; Fox, D. J.; Keith, T.; Al-Laham, M. A.; Peng, C. Y.; Nanayakkara, A.; Challacombe, M.; Gill, P. M. W.; Johnson, B.; Chen, W.; Wong, M. W.; Gonzalez, C.; Pople, J. A. *Gaussian 03*, revision C.02; Gaussian, Inc.: Wallingford, CT, 2004.
(43) Becke, A. D. *J. Chem. Phys.* **1993**, *98*, 5648–5652.
(44) (a) Perdew, J. P. *Phys. Rev. B* **1986**, *33*, 8822–8824. (b) Perdew, J. P. *Phys. Rev. B* **1986**, *34*, 7406.
(45) Lee, C.; Yang, W.; Parr, R. G. *Phys. Rev. B* **1988**, *37*, 785–789.
(46) (a) Perdew, J.; Burke, K.; Ernzerhof, M. *Phys. Rev. Lett.* **1996**, *77*, 3865–3868. (b) Perdew, J.; Burke, K.; Ernzerhof, M. *Phys. Rev. Lett.* **1997**, *78*, 1396–1396.

Table 2. $V^{IV}O^{2+}$ Stability Constants (log β_{pqr}) at 25.0 ± 0.1 °C and I = 0.20 M (KCl)[a]

class	ligand	VOLH	VOL	VOL_2	VOL_2H_{-1}	$(VOLH_{-1})_2$	$VOLH_{-2}$	ref.
A	3-mepicH		6.54(1)	11.63(1)		6.05(3)		this work
A	1-iqcH		6.14(2)	10.91(1)		4.67(4)		this work
A	2-pyacH		4.05(1)	7.88(2)		0.58(8)		this work
B	picH		6.66	12.11	5.13	6.15		50
B	fusarH		6.83(2)	12.71(1)	5.61(2)	7.13(3)		this work
B	3-iqcH		6.68(1)	11.86(2)	5.14(2)	6.08(8)		this work
C	6-mepicH	7.27	5.13	9.28		3.25	−6.56	51
C	6-me-2,3-$pdcH_2$	7.61(4)	4.56(1)	11.22(1)		1.83(3)	−7.05(4)	this work
C	quinH		5.45(1)	10.22(2)				this work
C	kynurH [b]		9.53(3)	18.24(2)				this work

[a] The uncertainties (σ values) are given in parentheses. [b] Values measured in a mixture H_2O/DMSO 50:50 v/v.

BHandHLYP functional in the calculation of ^{51}V hyperfine coupling constant along the z axis on 22 representative $V^{IV}O^{2+}$ complexes with different charges, geometries, and coordination modes was recently tested, with a mean deviation from the experimental value of $|A_z|$ of 2.7%.[47]

All the geometries of the $V^{IV}O^{2+}$ complexes investigated were first pre-optimized at the B3P86/sto-3g level and further optimized at the level of theory B3P86/6-311g in the gas phase. For all the structures, minima were verified through frequency calculations. The energy of the possible bis chelated species formed in water by 3-mepicH, picH, and 6-mepicH (Table 8) was calculated at the B3P86/6-311g level of theory within the framework of the polarizable continuum model (PCM).[48]

The optimized structures in the gas phase were used to predict the ^{51}V hyperfine coupling constants (A_{iso}, A_x, A_y, and A_z) and the stretching frequencies (ν) measurable from EPR and IR spectra. A_{iso}, A_x, A_y, and A_z were simulated at the BHandHLYP/6-311g(d,p) level of theory; $A_{x,y,z}$ were calculated as sum of the isotropic Fermi contact (A^{iso}) and the anisotropic or dipolar hyperfine interaction ($A^{D}_{x,y,z}$): $A_{x,y,z} = A^{iso} + A^{D}_{x,y,z}$. The percent deviation from the absolute experimental value, $|A_z|^{exptl}$, was calculated as $100[(|A_z|^{calcd} - |A_z|^{exptl})/|A_z|^{exptl}]$ (Table 7). The stretching frequency of V=O bond ($\nu_{V=O}$) was simulated at the B3P86/6-311g, B3LYP/6-311g, and PBE/6-311g levels of theory, respectively.

The analysis of molecular orbital (MO) composition in terms of atomic orbitals was performed using the AOMix program (revision 6.46).[49]

Results and Discussion

(1). Ligands. The protonation constants of the 10 derivatives are listed in Table 1. All the ligands have two titrable protons in water and can be indicated in the fully protonated form as H_2L^+, except 6-methyl-2,3-pyridindicarboxylic acid (H_3L^+). For H_2L^+ ligands the two protons belong to carboxylic group -COOH and to protonated aromatic nitrogen -NH^+. The values for picH and 6-mepicH were taken from the literature,[50,51] and those for kynurH were determined in a mixture H_2O/DMSO 50:50 v/v because of the low solubility of the ligand in water.

The pK_a values for the deprotonation of the carboxylic group range from 1.20 (3-mepicH) to 2.76 (2-pyacH). The second pK_a, attributable to the deprotonation of pyridine-N or quinoline-N, varies from 4.89 (quinH) to 5.78 (fusarH); such values are comparable with those reported in the literature for pyridine (5.23) and quinoline (4.90).[52]

The higher basicity of the pyridine-N in 6-mepicH, 6-me-2,3-$pdcH_2$, fusarH and 2-pyacH with respect to picH can be explained by the electron-releasing effect of the alkyl groups.

(2). Behavior in Aqueous Solution. (a). Class A. Class A ligands show a simple behavior with the formation of mono and bis chelated species through the donor set (N, COO^-). The stability constants and EPR parameters for $V^{IV}O^{2+}$ complexes are listed in Tables 2 and 3.

The species distribution diagram and EPR spectra recorded as a function of pH for the system with 3-methylpicolinic acid are shown in Figures 1 and 2.

At acid pH values a mono chelated species of composition $[VOL]^+$ is formed (**I** in Figure 2), with EPR parameters suggesting the coordination of the aromatic-N and carboxylate-O in a five-membered chelate ring: g_z values are in the range 1.938−1.942 and A_z in the range 172−173 × 10^{-4} cm^{-1} (Table 3). The attribution of the donor set was confirmed by the "additivity rule", which affirms that for a $V^{IV}O^{2+}$ complex the value of the ^{51}V isotropic hyperfine coupling constant measured on a frozen sample (A_z) can be calculated from the sum of the contributions of each equatorial donor:[53−55]

$$A_z = \sum_{i=1}^{4} A_z(\text{donor } i) = A_z(\text{donor 1}) + A_z(\text{donor 2}) + A_z(\text{donor 3}) + A_z(\text{donor 4}) \quad (1)$$

The hyperfine coupling constants measured for $[VOL]^+$ species agree well with those expected for a [(N, COO^-); H_2O; H_2O] coordination mode (174 × 10^{-4} cm^{-1}). The values of log β for $[VOL]^+$ formation are 6.54, 6.14, and

(47) Micera, G.; Garribba, E. *Dalton Trans.* **2009**, 1914–1918.
(48) (a) Miertus, S.; Scrocco, E.; Tomasi, J. *Chem. Phys.* **1981**, *55*, 117–129. (b) Miertus, S.; Tomasi, J. *Chem. Phys.* **1982**, *65*, 239–245. (c) Cossi, M.; Barone, R.; Cammi, R.; Tomasi, J. *Chem. Phys. Lett.* **1996**, *255*, 327–335.
(49) (a) Gorelsky, S. I. *AOMix program*; University of Ottawa: Ottawa, Ontario, Canada, 2009; http://www.sg-chem.net. (b) Gorelsky, S. I.; Lever, A. B. P. *J. Organomet. Chem.* **2001**, *635*, 187–196.
(50) Kiss, E.; Petrohan, K.; Sanna, D.; Garribba, E.; Micera, G.; Kiss, T. *Polyhedron* **2000**, *19*, 55–61.
(51) Kiss, E.; Garribba, E.; Micera, G.; Kiss, T.; Sakurai, H. *J. Inorg. Biochem.* **2000**, *78*, 97–108.
(52) Dissociation constants of organic acids and bases. In *CRC Handbook of Chemistry and Physics*, Internet Version 2005; Lide, D. R., Ed.; CRC Press: Boca Raton, FL, 2005; http://www.hbcpnetbase.com.
(53) Chasteen, N. D. In *Biological Magnetic Resonance*; Berliner, L. J., Reuben, J., Eds.; Plenum Press: New York, 1981; Vol. *3*, pp 53−119.
(54) Smith, T. S.; LoBrutto, R.; Pecoraro, V. L. *Coord. Chem. Rev.* **2002**, *228*, 1–18.
(55) Garribba, E.; Lodyga-Chruscinska, E.; Micera, G.; Panzanelli, A.; Sanna, D. *Eur. J. Inorg. Chem.* **2005**, 1369–1382, and references therein.

Table 3. Anisotropic EPR Parameters and Donor Sets for $V^{IV}O^{2+}$ Complexes in Aqueous Solution

ligand	complex	g_z	A_z[a]	donor set
3-mepicH	$[VOL]^+$	1.938	173	(N, COO^-); H_2O; H_2O
	$[VOL_2]$	1.946	162	(N, COO^-); (N, COO^-)
1-iqcH	$[VOL]^+$	1.939	173	(N, COO^-); H_2O; H_2O
	$[VOL_2]$	1.945	161	(N, COO^-); (N, COO^-)
2-pyacH	$[VOL]^+$	1.942	172	(N, COO^-); H_2O; H_2O
	$[VOL_2]$	1.951	162	(N, COO^-); (N, COO^-)
picH	$[VOL]^+$	1.939	175	(N, COO^-); H_2O; H_2O
	cis-$[VOL_2(H_2O)]$	1.945	165	(N, COO^-); (N, COO^-_{ax}); H_2O
	cis-$[VOL_2(OH)]^-$	1.947	160	(N, COO^-); (N, COO^-_{ax}); OH^-
fusarH	$[VOL]^+$	1.938	173	(N, COO^-); H_2O; H_2O
	cis-$[VOL_2(H_2O)]$	1.946	165	(N, COO^-); (N, COO^-_{ax}); H_2O
	cis-$[VOL_2(OH)]^-$	1.947	160	(N, COO^-); (N, COO^-_{ax}); OH^-
3-iqcH	$[VOL]^+$	1.938	173	(N, COO^-); H_2O; H_2O
	cis-$[VOL_2(H_2O)]$	1.945	164	(N, COO^-); (N, COO^-_{ax}); H_2O
	cis-$[VOL_2(OH)]^-$	1.947	160	(N, COO^-); (N, COO^-_{ax}); OH^-
6-mepicH	$[VOLH]^{2+}$	1.933	177	COO^-; H_2O; H_2O; H_2O
	$[VOL]^+$	1.939	168	(N, COO^-); H_2O; H_2O
	$[VOL_2]$	1.943	161	(N, COO^-); (N, COO^-)
	trans-$[VOL_2(H_2O)]$	1.949	149	(N, COO^-); (N, COO^-); H_2O^{ax}
6-me-2,3-pdcH_2	$[VOLH]^+$	1.933	177	COO^-; H_2O; H_2O; H_2O
	[VOL]	1.938	168	(N, COO^-); H_2O; H_2O
	$[VOL_2]^{2-}$	1.942	160	(N, COO^-); (N, COO^-)
	trans-$[VOL_2(H_2O)]^{2-}$	1.950	147	(N, COO^-); (N, COO^-); H_2O^{ax}
quinH	$[VOL]^+$	1.939	167	(N, COO^-); H_2O; H_2O
	$[VOL_2]$	1.941	161	(N, COO^-); (N, COO^-)
	trans-$[VOL_2(H_2O)]$	1.949	149	(N, COO^-); (N, COO^-); H_2O^{ax}
kynurH [b]	$[VOL]^+$	1.940	166	(N, COO^-); H_2O; H_2O
	$[VOL_2]$	1.942	161	(N, COO^-); (N, COO^-)
	trans-$[VOL_2(H_2O)]$	1.951	148	(N, COO^-); (N, COO^-); H_2O^{ax}

[a] Measured in 10^{-4} cm^{-1}. [b] Parameters measured in a mixture H_2O/DMSO 50:50 v/v.

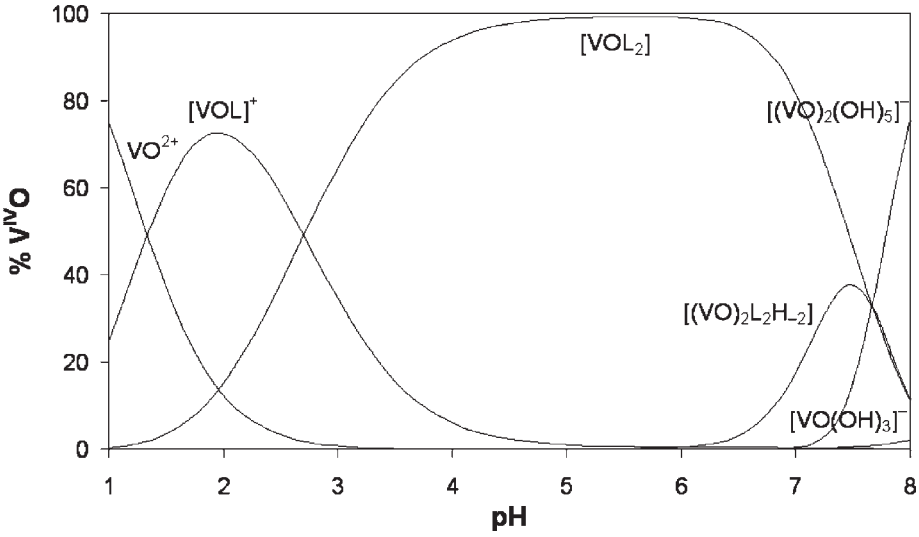

Figure 1. Species distribution diagram for the $V^{IV}O^{2+}$/3-mepicH system as a function of pH with a molar ratio of 1:4 and $V^{IV}O^{2+}$ concentration of 1 mM.

4.05 for 3-mepicH, 1-iqcH and 2-pyacH; the "basicity-adjusted" stability constants, which take into account the difference in basicity of the coordinating donors, for the reaction $VO^{2+} + HL \rightarrow [VOL]^+ + H^+$ (1.36, 1.10 and −1.66, respectively) suggest that the stability of mono chelated complex formed by 2-pyacH is about 3 orders of magnitude lower than 3-mepicH and 1-iqcH, because of the larger size of the chelated ring (six- instead of five-membered).

In the experimental conditions used, $[VOL]^+$ transforms into the bis chelated species $[VOL_2]$ ((a) in Scheme 1 and **II** in Figure 2). For these complexes the A_z value is in the range $161-162 \times 10^{-4}$ cm^{-1}, consistent with the coordination mode 2×(N, COO^-). The log β values for $[VOL_2]$ are 11.63, 10.91, and 7.88 for 3-mepicH, 1-iqcH, and 2-pyacH, respectively, corresponding to the "basicity-adjusted" stability constants of −0.09, −0.27, and −1.88 for the reaction $[VOL]^+ + HL \rightarrow [VOL_2] + H^+$: in this case too, the value for 2-pyacH is 2 orders of magnitude lower than the other ligands.

Above pH 7 for 1-iqcH and 3-mepicH and around pH 6 for 2-pyacH, one of the ligand molecules is replaced by OH^- ion with the formation of an EPR-silent species $[(VO)_2L_2H_{-2}]$ (or $[(VO)_2L_2(OH)_2]$). This is consistent with the principle established by Felcman and Da Silva that the hydrolysis of a $V^{IV}O^{2+}$ complex with two accessible

adjacent equatorial sites gives usually an EPR-silent, di-μ-hydroxido bridged dinuclear species.[56]

(b). Class B. Ligands belonging to class B form mono-, bis chelated, and hydrolytic species with $V^{IV}O^{2+}$ ion (Table 2). The distribution curves for the complexes formed by fusaric acid as a function of pH are depicted in Figure 3.

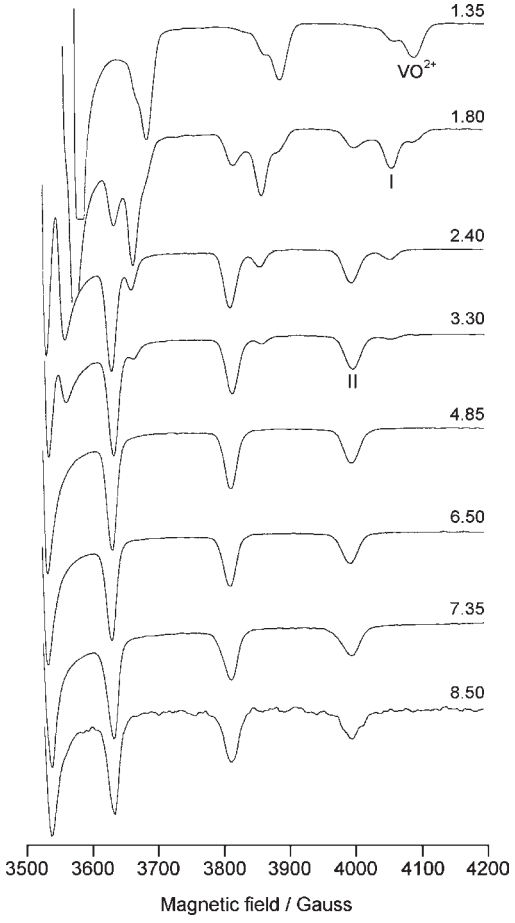

Figure 2. High field region of the X-band anisotropic EPR spectra recorded at 100 K as a function of pH on an aqueous solution of $V^{IV}O^{2+}$/3-mepicH system with a molar ratio of 1:4 and $V^{IV}O^{2+}$ concentration of 4 mM. $\mathbf{VO^{2+}}$, **I** and **II** indicate the resonances of $[VO(H_2O)_5]^{2+}$, $[VOL]^+$, and $[VOL_2]$ complexes, respectively.

The complexation starts with formation of $[VOL]^+$ at pH > 1 and $[VOL_2]$ at pH > 2. In $[VOL]^+$ (**I** in Figure 4), the pyridine-N or quinoline-N and carboxylate-O bind the metal ion forming five-membered chelate rings. EPR parameters of this species (g_z = 1.938−1.939 and A_z = 173−175 × 10^{-4} cm^{-1}, Table 3), similar to the analogous complexes formed by class A ligands, suggest the same binding mode. Also, the "basicity-adjusted" stability constants for the formation of $[VOL]^+$ are comparable: 1.47 for picH, 1.05 for fusarH, and 1.03 for 3-iqcH.

The bis complex $[VOL_2]$ (**II** in Figure 4) is the main species in the pH range 3−7. The values of the "basicity-adjusted" stability constants for the reaction $[VOL]^+ + HL \rightarrow [VOL_2] + H^+$ are 0.26, 0.10, and −0.45 for picH, fusarH, and 3-iqcH, respectively.

Potentiometric and EPR data (g_z = 1.945−1.946 and A_z = 164−165 × 10^{-4} cm^{-1}, Table 3) indicate the formation of *cis*-octahedral isomer ((b) in Scheme 1). Indeed, the deprotonation of $[VOL_2]$ takes place with pK in the range 6.72−7.10, a value sensibly lower than expected for a weakly bound axial water, suggesting the transformation of *cis*-$[VOL_2]$ (or *cis*-$[VOL_2(H_2O)]$) into *cis*-$[VOL_2H_{-1}]^-$ (or *cis*-$[VOL_2(OH)]^-$) with an OH^- ion rather a H_2O molecule in the equatorial plane.[50,57] Moreover, the A_z value agrees well with an *cis*-octahedral arrangement with two aromatic-N and one carboxylate-O on the equatorial plane, another COO^- group in the axial position and a water molecule occupying the fourth equatorial position (167.9 × 10^{-4} cm^{-1} predicted for [(N, COO^-); (N, COO^-_{ax}); H_2O] donor set and 169.9 × 10^{-4} cm^{-1} for [(N, COO^-); (N^{ax}, COO^-); H_2O]). Significantly, the A_z value of $[VOL_2]$ species is higher for class B than for class A by about 3−4 × 10^{-4} cm^{-1}, just the difference predicted by the "additivity rule" when a water-O replaces a carboxylate-O in the equatorial plane of $V^{IV}O^{2+}$.[55] This deduction is confirmed by the X-ray structures of solid $V^{IV}O^{2+}$ complexes formed by similar ligands provided with (N, COO^-) donor set: for example *cis*-$[VO(5MeOpic)_2(H_2O)]$,[27] *cis*-$[VO(5\text{-}i\text{PrOdipic})_2(H_2O)]$,[28] and $[VO(HDMCI)_2(H_2O)]$,[58] where 5MeOpicH, 5-*i*PrOdipicH, and H_2MDCI are 5-carbomethoxypicolinic acid, 5-carboisopropoxypicolinic acid, and 1-methyl-4,5-dicarboxyimidazole, respectively, for which the arrangement of the two ligand molecules is (equatorial-equatorial)

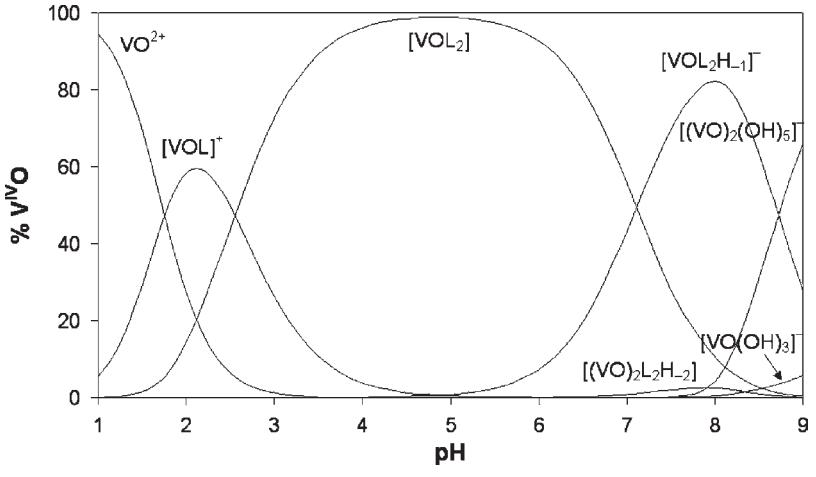

Figure 3. Species distribution diagram for the $V^{IV}O^{2+}$/fusarH system as a function of pH with a molar ratio of 1:4 and $V^{IV}O^{2+}$ concentration of 1 mM.

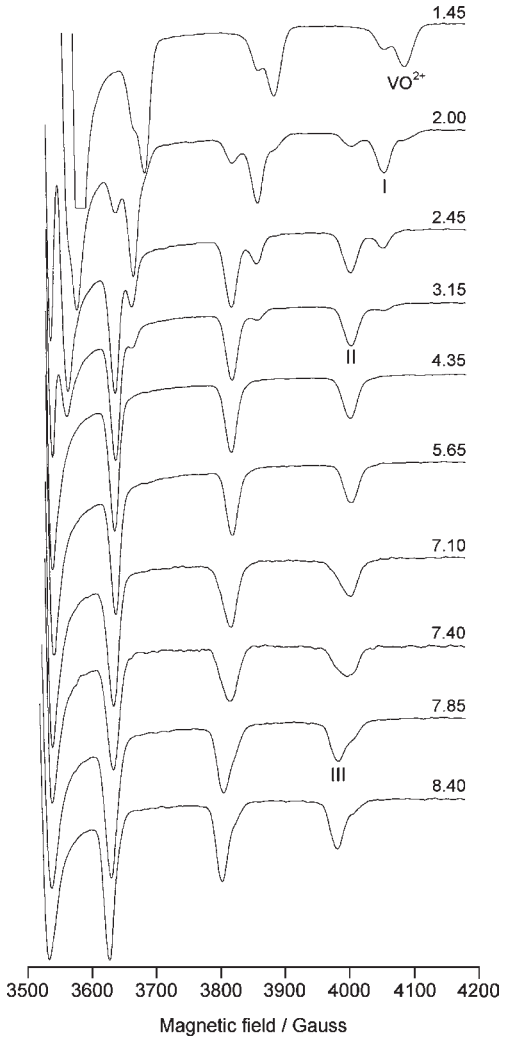

Figure 4. High field region of the X-band anisotropic EPR spectra recorded at 100 K as a function of pH on an aqueous solution of $V^{IV}O^{2+}$/fusarH system with a molar ratio of 1:2 and a $V^{IV}O^{2+}$ concentration of 4 mM. $\mathbf{VO^{2+}}$, **I**, **II**, and **III** indicate the resonances of $[VO(H_2O)_5]^{2+}$, $[VOL]^+$, *cis*-$[VOL_2(H_2O)]$, and *cis*-$[VOL_2(OH)]^-$ complexes, respectively.

and (equatorial-axial) and two aromatic-N are in the equatorial position.

The deprotonation of the water molecule yields a monohydroxido complex with *cis*-$[VOL_2(OH)]^-$ stoichiometry and [(N, COO^-); (N, COO^-_{ax}); OH^-)] donor set (**III** in Figure 4). This transformation is accompanied by a change of g_z and A_z values ($g_z = 1.947$ and $A_z = 160 \times 10^{-4}$ cm^{-1}, Table 3) and can be clearly distinguished by the EPR technique; in particular, on the basis of the "additivity rule", the replacement of a H_2O with a OH^- donor should reduce A_z by $5-6 \times 10^{-4}$ cm^{-1}.[55]

Above pH 9, stepwise displacement of the ligands by hydroxide ion results in the formation of di- and mononuclear complexes $[(VO)_2(OH)_5]^-$ and $[VO(OH)_3]^-$.

(c). Class C. For these ligands, the complexation process starts at pH $\sim$ 2 with the formation of species with composition VOLH for 6-mepicH and 6-me-2,3-pdcH_2 and VOL for quinH and kynurH. The lower basicity of quinoline-N than pyridine-N shifts the formation of [VOL] at more acid pH values for the two latter ligands and hinders the observation of VOLH. As an example, the distribution diagram for the species formed in the systems by 6-methyl-2,3-pyridindicarboxylic acid as a function of pH is shown in Figure 5.

The protonated species VOLH (**I** in Figure 6) in the systems formed by 6-mepicH and 6-me-2,3-pdcH_2 can be detected by EPR spectroscopy ($g_z = 1.933$ and $A_z = 177 \times 10^{-4}$ cm^{-1}, Table 3). These parameters support the coordination of one carboxylate group, with the pyridine-N being still protonated.

In the complex VOL (**II** in Figure 6), the pyridine-N and carboxylate-O of the ligand form a five-membered chelate ring (g_z in the range 1.938−1.940 and A_z in that $166-168 \times 10^{-4}$ cm^{-1}, Table 3).

The bis complex VOL_2 predominates in aqueous solution between pH 4 and 7. In this pH range, two sets of EPR signals are detected, with an intensity ratio almost constant, that suggest the existence of two species with identical 1:2 composition. The first complex exhibits $g_z = 1.941-1.943$ and $A_z = 160-161 \times 10^{-4}$ cm^{-1} ((a) in Scheme 1 and **III** in Figure 6) and the second $g_z = 1.949-1.951$ and $A_z = 147-149 \times 10^{-4}$ cm^{-1} ((c) in Scheme 1 and **IV** in Figure 6).

Usually, this type of situation has been interpreted in terms of an equilibrium between the square pyramidal and *cis*-octahedral form ((a) and (b), respectively, in Scheme 1).[51] Three main reasons allow one to rule out this explanation: (i) the A_z value for hypothetic *cis* species is significantly lower than that expected on the basis of the "additivity rule" ($A_z^{expct} \sim 169 \times 10^{-4}$ cm^{-1}) and experimentally measured for class B complexes ($A_z = 164-165 \times 10^{-4}$); (ii) the A_z value for the supposed penta-coordinated compound is anomalously low ($147-149 \times 10^{-4}$ cm^{-1}); (iii) the formation of monohydroxido species *cis*-$VOL_2(OH)$ upon deprotonation of the hypothetic *cis*-$VOL_2(H_2O)$ complex was not detected (neither by EPR spectroscopy nor pH-potentiometry), unlike to what is observed for class B ligands. It was recently demonstrated through the combined application of EPR and DFT methods that the behavior of ligands belonging to class C can be explained through the equilibrium between the penta-coordinated square pyramidal and hexa-coordinated *trans*-octahedral form (Scheme 1),[59] similar to what observed for Ni^{2+} ion for the equilibrium between the square pyramidal diamagnetic and the octahedral paramagnetic species with two water molecules in the axial position.[60] This hypothesis explains why the penta-coordinated species are characterized by A_z value similar to the analogous complexes formed by class A ligands ($161-162 \times 10^{-4}$ cm^{-1}, see above) and why the octahedral form is

(56) Felcman, J.; Fraústo da Silva, J. J. R. *Talanta* **1983**, *30*, 565–570.
(57) (a) Buglyó, P.; Kiss, E.; Fábián, I.; Kiss, T.; Sanna, D.; Garribba, E.; Micera, G. *Inorg. Chim. Acta* **2000**, *306*, 174–183. (b) Buglyó, P.; Kiss, T.; Kiss, E.; Sanna, D.; Garribba, E.; Micera, G. *J. Chem. Soc., Dalton Trans.* **2002**, 2275–2282. (c) Garribba, E.; Micera, G.; Sanna, D.; Chruscinska, E. *Inorg. Chim. Acta* **2003**, *348*, 97–106. (d) Garribba, E.; Micera, G.; Lodyga-Chruscinska, E.; Sanna, D. *Eur. J. Inorg. Chem.* **2006**, 2690–2700. (e) Rangel, M.; Leite, A.; Amorim, M. J.; Garribba, E.; Micera, G.; Lodyga-Chruscinska, E. *Inorg. Chem.* **2006**, *45*, 8086–8097.
(58) Smith, T. S., II; Root, C. A.; Kampf, J. W.; Rasmussen, P. G.; Pecoraro, V. L. *J. Am. Chem. Soc.* **2000**, *122*, 767–775.
(59) Gorelsky, S.; Micera, G.; Garribba, E. *Chem.—Eur. J.* **2010**, *16*, 8167–8180.

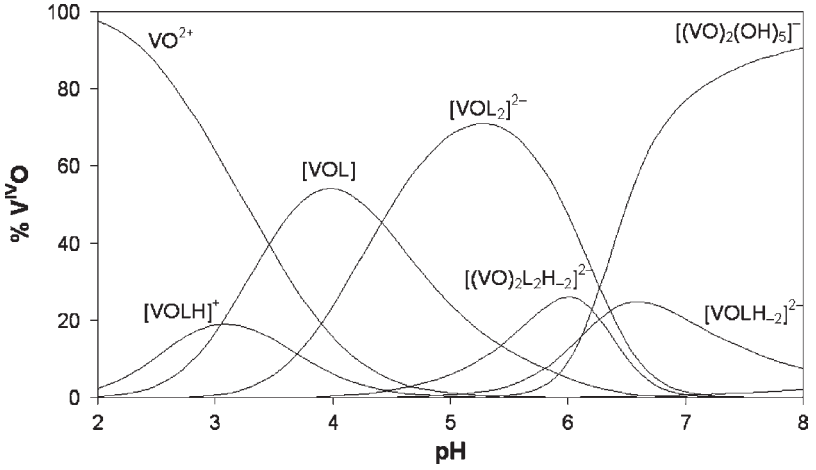

Figure 5. Species distribution diagram for the $V^{IV}O^{2+}$/6-me-2,3-pdcH_2 system as a function of pH with a molar ratio of 1:4 and $V^{IV}O^{2+}$ concentration of 1 mM.

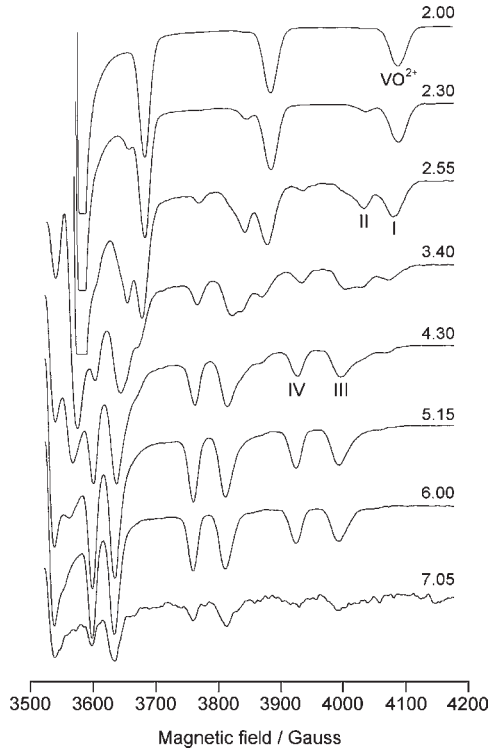

Figure 6. High field region of the X-band anisotropic EPR spectra recorded at 100 K as a function of pH on an aqueous solution of $V^{IV}O^{2+}$/6-me-2,3-pdcH_2 system with a molar ratio of 1:2 and $V^{IV}O^{2+}$ concentration of 4 mM. $\mathbf{VO^{2+}}$, **I**, **II**, **III**, and **IV** indicate the resonances of $[VO(H_2O)_5]^{2+}$, $[VOLH]^+$, [VOL], $[VOL_2]^{2-}$, and *trans*-$[VOL_2(H_2O)]^{2-}$ complexes, respectively.

characterized by a very low hyperfine coupling constant (see below, DFT Calculations Section).

The low solubility of VOL_2 species for 6-mepicH, quinH, and kynurH causes the precipitation of a solid compound from the aqueous solution. For this reason, with kynurenic acid it is necessary to use a mixture H_2O/DMSO 50:50 v/v.

Deprotonation and dimerization of the complex VOL occur in all the systems, and an EPR-silent di-μ-hydroxido-bridged complex $(VO)_2L_2H_{-2}$, is formed. Above pH 8, the EPR signals become very weak, indicating the formation of oligonuclear hydroxido-bridged EPR-silent species.

The pH-potentiometric and spectral studies reveal that the methyl group in 6-methylpicolinic and 6-methyl-2,3-pyridindicarboxylic acid or the presence of a condensed phenyl ring in quinaldic and kynurenic acid has a marked effect on the $V^{IV}O^{2+}$-binding capability of the ligands. The stability constants of class C complexes are significantly reduced as compared with those of classes A and B. For example, the "basicity-adjusted" stability constants for the formation of $[VOL]^+$ complexes are 1.36 for 3-methylpicolinic (class A), 1.47 for picolinic (class B), and -0.69 for 6-methylpicolinic acid (class C); analogously, the corresponding values for $[VOL_2]$ are -0.09 for 3-methylpicolinic (class A), 0.26 for picolinic (class B), and -1.67 for 6-methylpicolinic acid (class C). Thus, the results indicate that the complexes formed by class C ligands are about 2 orders of magnitude less stable than those of class A and B. This is presumably due to the increase of the hydrophobicity and steric hindrance of the methyl group or condensed phenyl ring. As mentioned above, the nature of the ligands also affects the geometry of the species and their spectral parameters.

(3). Behavior in the Solid State. (a). Class A. $[VO(3\text{-mepic})_2]$, $[VO(1\text{-iqc})_2]$, and $[VO(2\text{-pyac})_2]$ solid complexes exhibit similar thermogravimetric and spectroscopic (EPR, UV/vis and IR) behavior (Tables 4 and 5). Thermogravimetric analysis allows to rule out the presence of water bound to the metal ion. When dissolved in DMSO, DMF, or in a mixture CH_2Cl_2/toluene 50:50 v/v, they show EPR spectra indicative of a single species (Figure 7). The A_z value falls in the range $161-162 \times 10^{-4}$ cm^{-1}, in good agreement with the prediction of the "additivity rule",[53−55] and with the values measured in aqueous

(60) (a) Wilkins, R. G.; Yelin, R.; Margerum, D. W.; Weatherbum, D. C. *J. Am. Chem. Soc.* **1969**, *91*, 4326–4326. (b) Barbucci, R.; Fabbrizzi, L.; Paoletti, P.; Vacca, A. *J. Chem. Soc., Dalton Trans.* **1973**, 1763–1767. (c) Paoletti, P.; Fabbrizzi, L.; Barbucci, R. *Inorg. Chim. Acta Rev.* **1973**, *7*, 43–68. (d) Hinz, F. P.; Margerum, D. W. *Inorg. Chem.* **1974**, *13*, 2941–2949. (e) Anichini, A.; Fabbrizzi, L.; Paoletti, P.; Clay, R. M. *Inorg. Chim. Acta* **1977**, *24*, L21–L23, and references therein. (f) Iwamoto, E.; Kamamaru, T.; Sumitomo, Y.; Suzuki, Y.; Nishimoto, J. *J. Chem. Soc., Faraday Trans.* **1995**, *91*, 627–630.

Table 4. Anisotropic EPR Parameters of the $V^{IV}O^{2+}$ Solid Complexes Dissolved in DMSO[a]

	cis-$[VOL_2(H_2O)]$ [b]		$[VOL_2]$		*trans*-$[VOL_2(H_2O)]$ [b]	
	g_z	A_z	g_z	A_z	g_z	A_z
$[VO(3\text{-mepic})_2]$			1.945	162		
$[VO(1\text{-iqc})_2]$			1.944	161		
$[VO(2\text{-pyac})_2]$			1.950	162		
cis-$[VO(pic)_2(H_2O)]$	1.944	165				
cis-$[VO(fusar)_2(H_2O)]$	1.945	164				
cis-$[VO(3\text{-iqc})_2(H2O)]$	1.945	165				
$[VO(6\text{-mepic})_2]$			1.943	162	1.949	149
trans-$[VO(quin)_2(H_2O)]$			1.941	162	1.950	149
trans-$[VO(kynur)_2(H_2O)]$[b]			1.942	163	1.951	149

[a] A_z measured in 10^{-4} cm^{-1}. [b] The replacement of the water molecule by DMSO cannot be ruled out and must be taken into account.

Table 5. Electronic Absorption and IR Parameters of the $V^{IV}O^{2+}$ Solid Complexes

complex	λ_1 (nm)	λ_2 (nm)	λ_3 (nm)	λ_4 (nm)	$\nu_{V=O}$ (cm^{-1})	$\nu_{V=O}^{calcd}$ (cm^{-1})[a]
$[VO(3\text{-mepic})_2]$	385	560	740		966	1102, 1079, 1106
$[VO(1\text{-iqc})_2]$	375	515	735		970	1103, 1080, 1107
$[VO(2\text{-pyac})_2]$	410	540	740		976	1083, 1071, 1091
cis-$[VO(pic)_2(H_2O)]$	385	555	710		980	1039, 1025, 1041
cis-$[VO(fusar)_2(H_2O)]$	385	550	725		968	1039, 1027, 1046
cis-$[VO(3\text{-iqc})_2(H_2O)]$	380	535	745		983	1038, 1024, 1042
$[VO(6\text{-mepic})_2]$	395	505	700	855	918	1080, 1073, 1084
trans-$[VO(quin)_2(H_2O)]$	380	675	870		973	1071, 1063, 1076
trans-$[VO(kynur)_2(H_2O)]$	390	570	825		987	1072, 1064, 1078

[a] $\nu_{V=O}$ calculated at the B3P86/6-311g, B3LYP/6-311g, and PBE/6-311g levels of theory, respectively.

solution (Table 3). These values suggest a tetragonal geometry and a square pyramidal arrangement of the bidentate ligands and are comparable with those measured in DMSO (160×10^{-4} cm^{-1}) and in a CH_2Cl_2/toluene mixture (161×10^{-4} cm^{-1}) for [VO(8-quinolinecarboxylato)$_2$], for which an analogous $2\times(N, COO^-)$ coordination mode is reported.[57c]

The stretching frequency for V=O bond in the range 966−976 cm^{-1} and the electronic absorption spectra with three bands are typical for penta-coordinated, square pyramidal $V^{IV}O^{2+}$ species.[61]

(b). Class B. The presence of a water molecule strongly bound to the metal ion in *cis*-$[VO(pic)_2(H_2O)]$, *cis*-$[VO(fusar)_2(H_2O)]$, and *cis*-$[VO(3\text{-iqc})_2(H_2O)]$ is supported by the thermal behavior of the complexes: the water molecule is lost only above 150 °C, differently from simple hydration water that is usually lost just above room temperature.

As discussed above, in aqueous solution they are *cis*-octahedral with the two ligand molecules in an (equatorial-equatorial) and (equatorial-axial) arrangement with respect to V=O bond. The same structure is retained in the solid state, as supported by the results of Gätjens et al.,[27,28] who have determined the X-ray crystal structure of the bis chelated complexes formed by two derivatives of picolinic acid, 5-carbomethoxypicolinic and 5-carboisopropoxypicolinic acid. These compounds have a water molecule in the equatorial plane at 2.016 and 2.017 Å from vanadium and a carboxylate group at 2.122 and 2.129 Å as the axial donor. Orvig and co-workers, before us, proposed without the support of a X-ray determination the *cis* arrangement for $[VO(pic)_2(H_2O)]$.[62]

EPR spectra in DMSO, in DMF, and in a mixture CH_2Cl_2/toluene 50:50 v/v show the presence of only one species. A_z values in the range 164−165 $\times$ 10^{-4} cm^{-1}, higher by about 3×10^{-4} cm^{-1} than those of the complexes formed by class A ligands, support that the *cis*-octahedral arrangement is retained; such an increase in A_z (see Figure 7) is due to the replacement of an equatorial carboxylate-O by an oxygen donor belonging to a water or a solvent (DMSO or DMF) molecule. The electronic spectrum is characterized by three absorption band, the first in the range 380−385 nm, the second in the range 535−555 nm, and the third in the range 710−745 nm; $\nu_{V=O}$ frequency falls between 968 and 983 cm^{-1} (Table 5).

(c). Class C. Bis chelated $V^{IV}O^{2+}$ solid compounds for class C ligands can be anhydrous (6-mepicH) or have a water molecule coordinated to $V^{IV}O^{2+}$ in their stoichiometry (quinH, kynurH); therefore, the stoichiometry is $[VO(6\text{-mepic})_2]$, $[VO(quin)_2(H_2O)]$ and $[VO(kynur)_2(H_2O)]$.

In the literature, the X-ray structures of $V^{IV}O^{2+}$ complexes formed by quinaldic and ethylpicolinic (6-etpicH) acid are reported, *trans*-$[VO(quin)_2(H_2O)]$[63] and *trans*-$[VO(6\text{-etpic})_2(H_2O)]$.[25] In both species, the vanadium atom has a distorted octahedral coordination geometry, involving the two oxygen donors of oxido and aqua ligands in *trans* position with respect each other and two carboxylate-O and two pyridine-N in the equatorial plane. The distance between vanadium and water-O is 2.29 and 2.28 Å,[25,63] indicating a significant interaction. For *trans*-$[VO(6\text{-etpic})_2(H_2O)]$ the electronic absorption

(61) Selbin, J. *Chem. Rev.* **1965**, *65*, 153–175.
(62) Melchior, M.; Thompson, K. H.; Jong, J. M.; Rettig, S. J.; Shuter, E.; Yuen, V. G.; Zhou, Y.; McNeill, J. H.; Orvig, C. *Inorg. Chem.* **1999**, *38*, 2288–2293.
(63) Okabe, N.; Muranishi, Y. *Acta Crystallogr., Sect. E* **2002**, *58*, m287–m289.

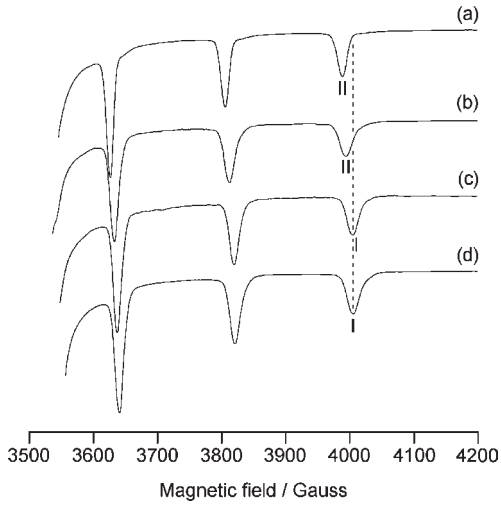

Figure 7. High field region of the X-Band anisotropic EPR spectra recorded at 100 K on the $V^{IV}O^{2+}$ solid complexes dissolved in DMSO: (a) $[VO(2\text{-pyac})_2]$, (b) $[VO(1\text{-iqc})_2]$, (c) *cis*-$[VO(3\text{-iqc})_2(H_2O)]$, and (d) *cis*-$[VO(pic)_2(H_2O)]$. **I** and **II** indicate the resonances of *cis*-octahedral and square pyramidal species, respectively, and the dotted line the position of $M_I = 7/2$ transition for *cis*-octahedral complexes.

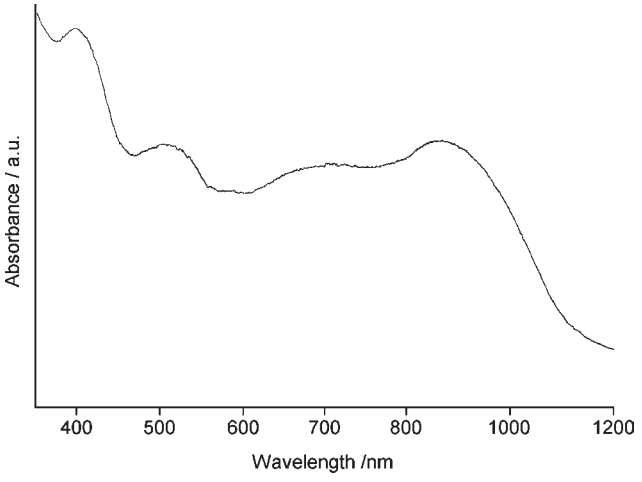

Figure 8. Electronic absorption spectrum of $[VO(6\text{-mepic})_2]$ recorded with the diffuse reflectance technique.

spectrum in DMSO is reported, with three bands centered at 740, 605, and 350 nm.[25]

The electronic absorption spectra of the three compounds are rather different (Table 5). $[VO(6\text{-mepic})_2]$ shows four bands of comparable intensity (Figure 8), which suggest the loss of the degeneracy of the energy levels associated to the d_{xz} and d_{yz} orbitals as a consequence of the distortion of the square pyramidal structure toward the trigonal bipyramid.[64,65] On the contrary, the spectra of *trans*-$[VO(quin)_2(H_2O)]$ and *trans*-$[VO(kynur)_2(H_2O)]$ are characterized by three bands, suggesting a more regular structure of the equatorial plane because of the axial coordination of the water molecule, that hinders the distortion of the complexes. These suppositions were confirmed by DFT calculations (see below).

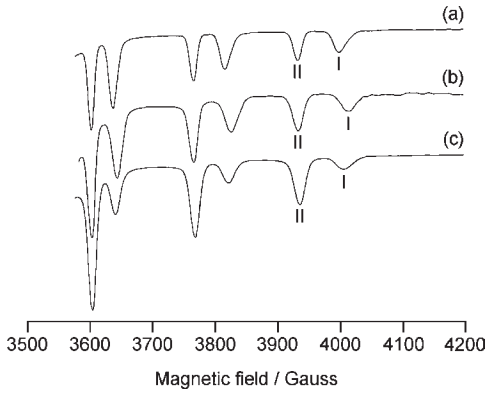

Figure 9. High field region of the X-Band anisotropic EPR spectra recorded at 100 K on the $V^{IV}O^{2+}$ solid complexes dissolved in DMSO. (a) $[VO(6\text{-mepic})_2]$, (b) *trans*-$[VO(kynur)_2(H_2O)]$, and (c) *trans*-$[VO(quin)_2(H_2O)]$. **I** and **II** indicate the resonances of square pyramidal and *trans*-octahedral species, respectively.

$[VO(6\text{-mepic})_2]$, *trans*-$[VO(quin)_2(H_2O)]$, and *trans*-$[VO(kynur)_2(H_2O)]$ show a peculiar EPR behavior when they are dissolved in DMSO or H_2O/DMSO mixtures. Indeed, the compounds undergo the same square pyramidal-octahedral equilibrium observed in aqueous solution. Whereas the A_z values for penta-coordinated species (**I** in Figure 9) are in agreement with those predicted by the "additivity rule" for a square pyramidal complexes with $2\times(N, COO^-)$ donor set and comparable with those displayed by compounds formed by class A ligands, the *trans*-octahedral species exhibit A_z of 149×10^{-4} cm^{-1} (Table 4), significantly lower than predicted.

Sakurai and co-workers report that EPR spectra of $[VO(6\text{-mepic})_2]$ and *trans*-$[VO(6\text{-etpic})_2(H_2O)]$ species dissolved in DMSO show two different species at room and liquid nitrogen temperature, with A_z values of $162-164 \times 10^{-4}$ cm^{-1} and $150-151 \times 10^{-4}$ cm^{-1},[25] very similar to those measured in this work.

Interestingly, whereas in DMSO and H_2O the square pyramidal and *trans*-octahedral species coexist, when $[VO(6\text{-mepic})_2]$ is dissolved in a mixture of non-coordinating solvents, like CH_2Cl_2/toluene 50:50 v/v, only the resonances of square pyramidal complexes are detected (trace a in Figure 10). On the contrary, in DMF the *trans*-octahedral species $[VO(6\text{-mepic})_2(dmf)]$ is strongly favored (trace c in Figure 10). EPR spectra of $[VO(6\text{-mepic})_2]$ and *trans*-$[VO(6\text{-mepic})_2(dmf)]$ are rhombic with three g ($g_z < g_x \neq g_y$) and three A ($A_z > A_x \neq A_y$) values ($g_x = 1.979$, $g_y = 1.973$, $g_z = 1.942$, $A_x = 41.4 \times 10^{-4}$ cm^{-1}, $A_y = 47.6 \times 10^{-4}$ cm^{-1}, $A_z = 161.5 \times 10^{-4}$ cm^{-1} for $[VO(6\text{-mepic})_2]$, and $g_x = 1.981$, $g_y = 1.972$, $g_z = 1.949$, $A_x = 39.6 \times 10^{-4}$ cm^{-1}, $A_y = 49.1 \times 10^{-4}$ cm^{-1}, $A_z = 148.5 \times 10^{-4}$ cm^{-1} for *trans*-$[VO(6\text{-mepic})_2(dmf)]$).

A distinctive feature of $[VO(6\text{-mepic})_2]$ with respect to *trans*-$[VO(quin)_2(H_2O)]$ and *trans*-$[VO(kynur)_2(H_2O)]$ is the significantly lower stretching frequency of the V=O bond (918 vs $973-987$ cm^{-1}, Table 5). A low value of $\nu_{V=O}$ for $[VO(6\text{-mepic})_2]$ has been already reported.[13] These frequencies must be compared with those of the compounds formed by class A and B ligands, which fall in the range $966-983$ cm^{-1}, as expected for a tetragonal $V^{IV}O^{2+}$ species. This may indicate that V=O in *trans*-$[VO(6\text{-mepic})_2]$ is weaker than normally or the solid state interaction between the vanadyl oxygen of one

(64) Cornman, C. R.; Geisre-Bush, K. M.; Rowley, S. R.; Boyle, P. D. *Inorg. Chem.* **1997**, *36*, 6401–6408.
(65) Garribba, E.; Micera, G.; Panzanelli, A.; Sanna, D. *Inorg. Chem.* **2003**, *42*, 3981–3987.

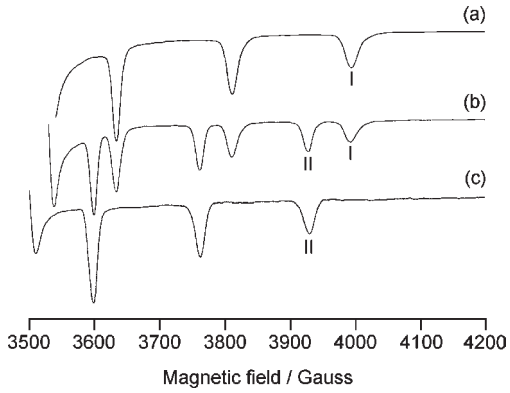

Figure 10. High field region of the anisotropic X-Band EPR spectra recorded at 100 K on $[VO(6\text{-mepic})_2]$ dissolved in several solvents: (a) CH_2Cl_2/toluene 50:50 v/v, (b) DMSO, and (c) DMF. **I** and **II** indicate the resonances of the square pyramidal and *trans*-octahedral species, respectively.

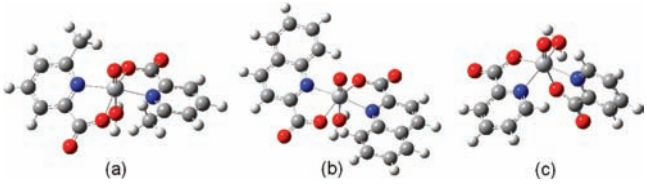

Figure 11. Structures of (a) *trans*-$[VO(6\text{-mepic})_2(H_2O)]$, (b) *trans*-$[VO(quin)_2(H_2O)]$, and (c) *cis*-$[VO(pic)_2(H_2O)]$, optimized at the B3P86/6-311g level of theory.

molecule with the open axial site of vanadium in another molecule.[66] DFT calculations allow to choose the second possibility and indicate that in the gas phase the strength of the V=O bond in $[VO(6\text{-mepic})_2]$ is similar to that in *trans*-$[VO(quin)_2(H_2O)]$ and *trans*-$[VO(kynur)_2(H_2O)]$; this confirms, moreover, the significant tendency of class C complexes to receive electronic density in the axial position and to coordinate a sixth ligand.

(4). DFT Calculations. (a). Optimization of the Structures. The structure of the bis chelated complexes was optimized with Gaussian 03 at the B3P86/6-311g level of theory. It has been found that the hybrid exchange-correlation B3P86 is better than other functionals (B3PW91, TPSSh, PBE, TPSS, BPW91, BP86, VSXC, BLYP, and the most popular B3LYP) in the simulation of the geometry of first-row transition metal compounds.[67] These results were recently confirmed by the calculation at the B3P86/6-311g level of theory of 32 V=O, 45 V−O, and 40 V−N bond distances; the mean of the absolute value of Δd (where $\Delta d = d^{calcd} - d^{exptl}$) was 0.014, 0.032, and 0.024 Å, respectively (to be compared with 0.015, 0.037, and 0.033 Å for simulations at the level of theory B3LYP/6-311 g), corresponding to a percent deviation below 2%.[68]

The calculated structures for *trans*-$[VO(6\text{-mepic})_2(H_2O)]$, *trans*-$[VO(quin)_2(H_2O)]$, and *cis*-$[VO(pic)_2(H_2O)]$ (Figure 11) were compared with those of *trans*-$[VO(6\text{-etpic})_2(H_2O)]$,[25] *trans*-$[VO(quin)_2(H_2O)]$,[63] and *cis*-$[VO(5\text{-}i\text{PrOdipic})_2(H_2O)]$.[28] No square pyramidal structure formed by class A ligands is available in the literature. The comparison between the calculated and experimental structures shows a good agreement (Table 6): the mean value of the absolute deviation for bond lengths and angles is 0.8 and 1.7% for *trans*-$[VO(6\text{-mepic})(H_2O)]$, 0.7 and 1.3% for *trans*-$[VO(quin)_2(H_2O)]$, and 1.4 and 3.9% for *cis*-$[VO(pic)_2(H_2O)]$. Also the axial $V-OH_2$ distance, incorrectly estimated by the B3LYP functional,[59] is satisfactorily predicted.

(b). Prediction of the EPR Parameters. Over the past years, DFT methods have been widely applied to the calculation of EPR parameters of transition metal complexes,[69] and $V^{IV}O^{2+}$ species.[70] Recently, ^{51}V hyperfine coupling constant (A_z) was calculated with Gaussian 03 software for 22 representative $V^{IV}O^{2+}$ complexes having different charge, geometry, and coordination mode at the BHandHLYP/6-311g(d,p) level of theory with a mean deviation of 2.7% from the experimental values.[47] The use of half-and-half hybrid functionals like BHandHLYP and BHandH, that allows to treat core shell spin polarization, seems to be necessary to obtain a satisfactory agreement with the experimental results.

The calculated and experimental EPR parameters are listed in Table 7.

From the examination of Table 7 several points must be noticed. (i) All the $|A_z|$ values are underestimated, suggesting that the second-order spin−orbit contribution to $\boldsymbol{A}$ tensor must be probably considered;[70c] (ii) the percent deviations from $|A_z|^{exptl}$ are below 3% with a mean deviation of 2.2%; (iii) DFT methods predict a low value of $|A_z|$ for the *trans*-octahedral species with a water molecule coordinated in the axial position; (iv) the significant reduction of $|A_z|$ for such complexes can be mainly related to the decrease of $|A_{iso}|$ rather than the dipolar hyperfine term $A^D{}_z$ (see Experimental and Computational Section; for example, from $[VO(6\text{-mepic})_2]$ to *trans*-$[VO(6\text{-mepic})_2](H_2O)]$ $|A_{iso}|$ goes from 88.0 to 78.2×10^{-4} cm^{-1}, whereas $|A^D{}_z|$ from 68.1 to 66.3×10^{-4} cm^{-1}); (v) $|A_z|$ values calculated for square pyramidal and *cis*-octahedral species are in good agreement with the experimental ones. Therefore, as recently pointed out, the axial coordination of a sixth ligand in the axial position significantly reduces the value of $|A_z|$ and, in such cases, the "additivity rule" cannot be applied.[59]

Finally, DFT methods correctly predict the order of $|A_x - A_y|$ values that can be related to the x,y anisotropy: $|A_x - A_y|$(*trans*-octahedral) > $|A_x - A_y|$(square pyramidal) > $|A_x - A_y|$(*cis*-octahedral).

(c). Prediction of $\nu_{V=O}$. The prediction of harmonic vibrational frequencies on the basis of DFT methods has been rather extensively pursued.[71] Often, the frequencies

(66) Hamilton, D. E. *Inorg. Chem.* **1991**, *30*, 1670–1671, and references therein.

(67) (a) Bühl, M.; Kabrede, H. *J. Chem. Theory Comput.* **2006**, *2*, 1282–1290. (b) Bühl, M.; Reimann, C.; Pantazis, D. A.; Bredow, T.; Neese, F. *J. Chem. Theory Comput.* **2008**, *4*, 1449–1459.

(68) Micera, G.; Garribba, E. *J. Chem. Theory Comput.* **2011**, submitted.

(69) (a) *Calculation of NMR and EPR Parameters. Theory and Applications*; Kaupp, M., Buhl, M., Malkin, V. G., Eds.; Wiley-VCH: Weinheim, 2004. (b) Remenyi, C.; Reviakine, R.; Arbuznikov, A. V.; Vaara, J.; Kaupp, M. *J. Phys. Chem. A* **2004**, *108*, 5026–5033, and references therein. (c) Neese, F. *Coord. Chem. Rev.* **2009**, *253*, 526–573, and references therein.

(70) (a) Munzarová, M. L.; Kaupp, M. *J. Phys. Chem. B* **2001**, *105*, 12644–12652, and references therein. (b) Saladino, A. C.; Larsen, S. C. *J. Phys. Chem. A* **2003**, *107*, 1872–1878. (c) Neese, F. *J. Chem. Phys.* **2003**, *118*, 3939–3948. (d) Aznar, C. P.; Deligiannakis, Y.; Tolis, E. J.; Kabanos, T. A.; Brynda, M.; Britt, R. D. *J. Phys. Chem. A* **2004**, *108*, 4310–4321. (e) Saladino, A. C.; Larsen, S. C. *Catal. Today* **2005**, *105*, 122–133, and references therein.

(71) Koch, W.; Holthausen, M. C. *A Chemist's Guide to Density Functional Theory*, 2nd ed.; Wiley-VCH: Weinheim, 2001.

Table 6. Calculated[a] Structural Details for $V^{IV}O^{2+}$ Complexes Formed by Class B and C Ligands[b]

length/angle	[VO(6-mepic)$_2$(H$_2$O)]	[VO(6-etpic)$_2$(H$_2$O)][c]	[VO(quin)$_2$(H$_2$O)]	[VO(quin)$_2$(H$_2$O)][d]	[VO(pic)$_2$(H$_2$O)]	[VO(5-*i*PrOdipic)$_2$(H$_2$O)][e]
V=O	1.595	1.571	1.592	1.602	1.604	1.599
V−N	2.133	2.146, 2.153	2.155	2.139, 2.155	2.102, 2.164	2.107, 2.150
V−O	1.977	1.956, 2.001	1.978	1.981, 2.021	1.948, 2.094	1.989, 2.129
V−OH$_2$	2.300	2.283	2.248	2.251	2.085	2.018
O=V−N	96.2	94.4, 97.1	95.1	93.9, 94.0	100.8, 87.2	95.7, 90.8
O=V−O	106.3	100.7, 102.3	104.3	104.4, 100.4	107.9, 159.8	106.2, 164.6
O=V−OH$_2$	180.0	176.9	180.0	176.4	103.0	97.4
N−V−N	167.7	167.8	169.8	171.2	[f]	[f]
O−V−O	147.4	156.7	151.4	154.9	[f]	[f]

[a] Calculated at the B3P86/6-311g level of theory. [b] All the values given in Å and in degrees. [c] X-ray structure reported in ref 25. [d] X-ray structure reported in ref 64. [e] X-ray structure reported in ref 28. [f] Values not significant.

Table 7. Calculated (A^{calcd}) and Experimental (A^{exptl}) ^{51}V Hyperfine Coupling Constants for $V^{IV}O^{2+}$ Complexes[a]

complex	A_{iso}^{calcd}	A_x^{calcd}	A_y^{calcd}	A_z^{calcd}	A_x^{exptl}	A_y^{exptl}	A_z^{exptl}	dev. % [b]	$\lvert A_x-A_y\rvert^{calcd}$	$\lvert A_x-A_y\rvert^{exptl}$
[VO(3-mepic)$_2$]	−88.7	−50.6	−58.3	−157.2	−52.1	−56.8	−161.6	−2.7	7.7	4.7
[VO(1-iqc)$_2$]	−88.1	−49.9	−57.9	−156.6	−51.2	−56.8	−160.8	−2.6	8.0	5.6
[VO(2-pyac)$_2$]	−90.6	−53.7	−58.8	−159.5	−55.6	−55.6	−162.1	−1.6	5.1	0.0
cis-[VO(pic)$_2$(H$_2$O)]	−96.5	−62.0	−64.1	−163.5	−60.8	−60.8	−165.0	−0.9	2.1	0.0
cis-[VO(fusar)$_2$(H$_2$O)]	−96.2	−61.0	−64.2	−163.5	−60.2	−60.2	−164.7	−0.7	3.2	0.0
cis-[VO(3-iqc)$_2$]	−96.3	−61.7	−64.0	−163.4	−60.5	−60.5	−164.4	−0.6	2.2	0.0
[VO(6-mepic)$_2$]	−88.0	−49.2	−58.7	−156.1	−53.2	−58.8	−160.8	−2.9	9.5	5.6
trans-[VO(6-mepic)$_2$](H$_2$O)]	−78.2	−39.2	−50.9	−144.5	−42 [c]	−49 [c]	−149.0	−3.0	11.6	7.0
[VO(6-me-2,3-dipic)$_2$]$^{2-}$	−87.7	−48.9	−58.6	−155.7	−52.6	−59.0	−160.1	−2.8	9.7	6.4
trans-[VO(6-me-2,3-dipic)$_2$](H$_2$O)]$^{2-}$	−78.0	−39.0	−50.8	−144.1	−41 [c]	−50 [c]	−146.5	−1.6	11.9	9.0
[VO(quin)$_2$]	−88.4	−49.8	−58.9	−156.4	−52.8	−58.8	−160.9	−2.8	9.0	6.0
trans-[VO(quin)$_2$(H$_2$O)]	−78.3	−39.9	−50.7	−144.2	−41 [c]	−50 [c]	−148.7	−3.0	10.8	9.0
[VO(kynur)$_2$]	−88.6	−50.0	−59.1	−156.7	−52.9	−59.0	−161.1	−2.7	9.1	6.1
trans-[VO(kynur)$_2$(H$_2$O)]	−78.9	−40.6	−51.2	−144.9	−41 [c]	−50 [c]	−148.4	−2.3	10.6	9.0

[a] All the values given in 10^{-4} cm^{-1}. [b] Percent deviation from $\lvert A_z\rvert^{exptl}$, calculated as $100(\lvert A_z\rvert^{calcd} - \lvert A_z\rvert^{exptl})/\lvert A_z\rvert^{exptl}$. [c] Values measurable only approximately.

predicted by GGA functionals such as BP86 and PBE agree well with observed fundamentals with errors being usually below 10%.[69c] It has been shown that this good agreement arises from a cancellation of errors, the underestimation of harmonic frequencies on one hand and the neglect of anharmonicities in these calculations on the other.[72] Harmonic frequencies are better predicted by hybrid functionals but to explicitly calculate anharmonic corrections to harmonic vibrational frequencies is a very difficult task. Consequently, as observed in the literature,[69c] the systematic error cancellation that occurs with GGA functionals appears to be a fortunate coincidence and can be of great help in the assignment of the experimental spectra. In this work, the stretching frequency of the V=O bond was calculated with three different functionals (hybrids B3P86 and B3LYP, and GGA PBE) and the triple-ζ basis set 6-311g. The results are summarized in Table 5. On the whole, the data are comparable: all the three functionals used overestimate the value of $\nu_{V=O}$ and suggest that in the gas phase $\nu_{V=O}$ (class B) < $\nu_{V=O}$ (class C) < $\nu_{V=O}$ (class A). This order depends on the strength of the axial interaction and reflects the length of V=O bond (mean value of 1.585, 1.591, and 1.605 Å for classes A, C and B, respectively). Of course, it must be taken into account that the simulations were performed in the gas phase and factors that can be important in determining the experimental values of $\nu_{V=O}$, such as the secondary hydrogen-bondings between the coordinated ligands and the solvent, packing factors, and solid-state effects, were not included in the calculations. However, for [VO(6-mepic)$_2$] a wavenumber comparable to the other components of class C complexes was found, demonstrating that the low value of $\nu_{V=O}$ observed in the solid state is probably due to the interaction between the oxido-O with a vanadium atom of another molecule.

It must be pointed out that, unlike what is reported,[69c] the predictions of the PBE functional are slightly inferior than those of hybrid functionals (mean percent deviation of 11.0 for PBE, 10.4 for B3P86 and 9.1% for B3LYP) and that, among B3P86 and B3LYP, the second performs better than the first one. However, the percent deviation of about 10% is in agreement with the data in the literature.

(d). Relative Stability of Bis Chelated Complexes in Aqueous Solution. The relative stability of bis chelated complexes formed by the three classes of ligands can be evaluated calculating the Gibbs free energy in aqueous solution (ΔG^{tot}_{aq}) for reactions 2 and 3 for the formation of *trans*- and *cis*-octahedral species from the square pyramidal complex:

$$[VOL_2] + H_2O \rightarrow \textit{trans}\text{-}[VOL_2(H_2O)] \qquad (2)$$

$$[VOL_2] + H_2O \rightarrow \textit{cis}\text{-}[VOL_2(H_2O)] \qquad (3)$$

The value of ΔG^{tot}_{aq} can be separated into three parts: the electronic plus nuclear repulsion energy (ΔE^{ele}), the thermal contribution (ΔG^{therm}), and the solvation free energy ($\Delta(\Delta G^{solv})$), as given in eq 4. The thermal contribution was estimated using the ideal gas model and the calculated harmonic vibrational frequencies to determine

(72) Neugebauer, J.; Hess, B. A. *J. Chem. Phys.* **2003**, *118*, 7215–7225.

Table 8. Free Energy for the Reaction of Formation in the Gas Phase and in Water of *trans*-Octahedral and *cis*-Octahedral Species from the Square Pyramidal Complex[a,b]

Reaction	ΔE^{ele}	$\Delta G^{therm\,c}$	$\Delta G^{tot}{}_{gas}$	$\Delta(\Delta G^{solv})^{d}$	$\Delta G^{tot}{}_{aq}$
$[VO(3\text{-mepic})_2] + H_2O \rightarrow$ *trans*-$[VO(3\text{-mepic})_2(H_2O)]$	−54.6	55.5	0.9	1.9	2.8
$[VO(3\text{-mepic})_2] + H_2O \rightarrow$ *cis*-$[VO(3\text{-mepic})_2(H_2O)]$	−49.0	56.1	7.1	−3.8	3.3
$[VO(pic)_2] + H_2O \rightarrow$ *trans*-$[VO(pic)_2(H_2O)]$	−55.9	55.7	−0.2	−2.5	−2.7
$[VO(pic)_2] + H_2O \rightarrow$ *cis*-$[VO(pic)_2(H_2O)]$	−40.6	55.9	15.3	−19.8	−4.5
$[VO(6\text{-mepic})_2] + H_2O \rightarrow$ *trans*-$[VO(6\text{-mepic})_2(H_2O)]$	−53.4	50.9	−2.5	−0.5	−3.0
$[VO(6\text{-mepic})_2] + H_2O \rightarrow$ *cis*-$[VO(6\text{-mepic})_2(H_2O)]$	−15.9	49.0	33.1	−9.8	23.3

[a] All the energies in kJ mol^{-1}. [b] Calculations performed at the B3P86/6-311g level of theory. [c] Thermal contribution at 298 K with the zero-point energy included in the calculations. [d] PCM model used with water as solvent.

the correction due to zero point energy (ZPE) and to thermal population of the vibrational levels:

$$\Delta G^{tot}{}_{aq} = \Delta E^{ele} + \Delta G^{therm} + \Delta(\Delta G^{solv})) \quad (4)$$

The Gibbs free energy in the gas phase ($\Delta G^{tot}{}_{gas}$), instead, can be found by neglecting the term ($\Delta(\Delta G^{solv})$):

$$\Delta G^{tot}{}_{gas} = \Delta E^{ele} + \Delta G^{therm} \quad (5)$$

These calculations were applied to 3-methylpicolinic, picolinic, and 6-methypicolinic acid, chosen as representative ligands for classes A, B, and C. The results are reported in Table 8.

DFT calculations show that in the gas phase the order of stability of bis chelated species is square pyramidal ∼ *trans*-octahedral > *cis*-octahedral (class A), *trans*-octahedral ∼ square pyramidal ≫ *cis*-octahedral (class B), and *trans*-octahedral > square pyramidal ≫ *cis*-octahedral (class C). This order can be reversed in aqueous solution because of the free energy of solvation that in all the three cases favor *cis*-octahedral species; in particular, this is rather large for picH probably for the absence of the methyl groups. In good agreement with the spectroscopic data, the order of stability in aqueous solution is square pyramidal > *trans*-octahedral ∼ *cis*-octahedral (class A), *cis*-octahedral > *trans*-octahedral > square pyramidal (class B) and *trans*-octahedral > square pyramidal ≫ *cis*-octahedral (class C). Therefore, the greater stability of *cis*-$[VO(pic)_2(H_2O)]$ in water with respect to the two other possible species depends on its solvation energy. Moreover, it is noteworthy that the values of $\Delta(\Delta G^{solv})$ for 6-mepicH are somewhat smaller than those for picH, and this can be put in relation with the lower thermodynamic stability of its complexes discussed above (see Table 2).

It must be pointed out that DFT simulations yield only qualitative results, at least until more accurate methods are developed, and if on the one hand they can provide information on the relative stability of several species in aqueous solution on the other they are not able to predict their exact percent amount; for example, our calculations suggest that for 6-mepicH *trans*-octahedral species is more stable than the square pyramidal, whereas spectroscopic evidence indicate that in water a comparable amount of the two complexes exists (Figure 6).

(e). Electronic Structure and Molecular Orbitals Composition. The electronic structure of four representative species belonging to the three classes, $[VO(3\text{-mepic})_2]$ (class A), *cis*-$[VO(pic)_2(H_2O)]$ (class B), *trans*-$[VO(6\text{-mepic})_2(H_2O)]$, and $[VO(6\text{-mepic})_2]$ (class C), is shown in Scheme 2. For clarity, the energy of the molecular orbitals (MOs) is relative to highest occupied molecular orbital (HOMO), set as reference at 0.0 eV.

The analysis of the electronic structure and molecular orbital composition has been performed choosing a coordinate system in which the V=O bond occupies the z axis, the pyridine-N are oriented along the x axis, and the carboxylate-O along the y axis.

The examination of Scheme 2 suggests several observations: (i) in all the cases the vanadium-based d_{xy} orbital is at lower energy; (ii) the deviation from the perfect square pyramidal geometry decreases the effective symmetry of the species and causes the splitting of the d_{xz} and d_{yz} orbitals; (iii) among the d orbitals, d_{z^2} orbital is always at higher energy; (iv) the first four unoccupied MOs (lowest unoccupied molecular orbital (LUMO), LUMO+1, LUMO+2, and LUMO+3) are π^* orbitals of the two pyridine rings; (v) the energy order of the five V-d based MOs reflects that calculated by Ballhausen and Gray for a $V^{IV}O^{2+}$ complex with C_{4v} symmetry:[73] $d_{xy} < d_{xz} \sim d_{yz} < d_{x^2-y^2} < d_{z^2}$.

Some selected molecular orbital for *cis*-$[VO(pic)_2(H_2O)]$ is shown in Figure 12. The π interaction between the V-d_{xy} and O-p_x orbital of the two bound carboxylate-O reduces the vanadium character of the HOMO in the range 74−79%. The energy difference HOMO−LUMO is comparable in the four cases, around 4 eV. As noticed elsewhere,[59] the V-d_{xz} and V-d_{yz} based MOs (in red in Scheme 2) are engaged in a π bond with the O_{oxido}-p_x and O_{oxido}-p_y orbitals (Figure 12c and 12d); their energy separation, 0.14 eV for *cis*-$[VO(pic)_2(H_2O)]$, 0.18 eV for *trans*-$[VO(6\text{-mepic})_2(H_2O)]$, 0.27 eV for $[VO(3\text{-mepic})_2]$, and 0.55 eV for $[VO(6\text{-mepic})_2]$, reflects the degree of distortion of the equatorial plane toward the trigonal bipyramid, expressed by the trigonality index τ, defined as $(\beta-\alpha)/60$, where β and α are the angles formed by the two axial and two equatorial donors,[74] 1 for an ideal trigonal bipyramidal and 0 for a square pyramidal geometry (for example, τ is 0.476 for $[VO(6\text{-mepic})_2]$ and 0.167 for $[VO(3\text{-mepic})_2]$).

The V-$d_{x^2-y^2}$ (in green in Scheme 2) is antibonding between the vanadium and the equatorial donors, but its energy does not change significantly in the four cases. The V-d_{z^2} orbital (in blue in Scheme 2) is pushed up in energy after the interaction with the axial donor (carboxylate-O in *cis*-$[VO(pic)_2(H_2O)]$ and water-O in *trans*-$[VO(6\text{-mepic})_2(H_2O)]$) and is higher for hexa- than for penta-coordinated species of more than 0.5 eV. It must be also noticed that it

(73) Ballhausen, C. J.; Gray, H. B. *Inorg. Chem.* **1962**, *1*, 111–122.
(74) Addison, A. W.; Rao, T. N.; Reedijk, J.; van Rijn, J.; Verschoor, G. C. *J. Chem. Soc., Dalton Trans.* **1984**, 1349–1356.

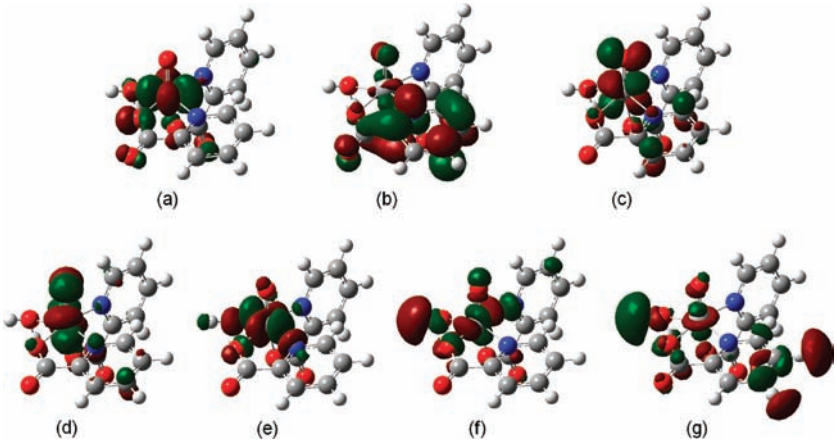

Figure 12. Molecular orbitals for *cis*-[VO(pic)$_2$(H$_2$O)]: (a) V-d$_{xy}$ (HOMO), (b) π^*_{pyr} (LUMO), (c) V-d$_{xz}$ (LUMO+4), (d) V-d$_{yz}$ (LUMO+5), (e) V-d$_{x^2-y^2}$ (LUMO+6), (f) V-4s (LUMO+7), and (g) V-d$_{z^2}$ (LUMO+9).

Scheme 2. Relative Energy Levels of the Most Representative Molecular Orbitals of [VO(3-mepic)$_2$], *cis*-[VO(pic)$_2$(H$_2$O)], *trans*-[VO(6-mepic)$_2$(H$_2$O)], and [VO(6-mepic)$_2$]

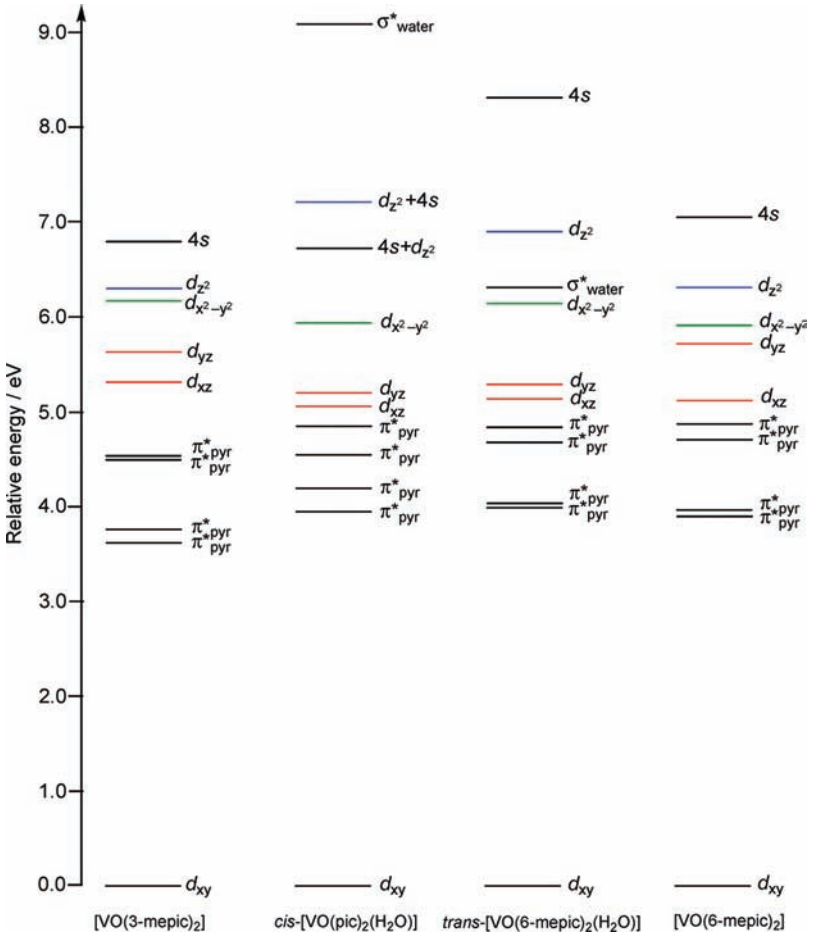

is strongly coupled with V-4s orbital in the case of *cis*-[VO(pic)$_2$(H$_2$O)].

(5). Biotransformation of Insulin-Enhancing $V^{IV}O^{2+}$ Compounds. The results obtained can applied to the possible biotransformation in the blood serum of these potent insulin-enhancing agents, in which class A, B, and C ligands behave as organic *carriers*. In particular, such processes are related to the thermodynamic stability of the bis chelated compounds and to their geometry in aqueous solution.[32] The strength of the three types of *carrier* is in the order class C $\ll$ class A $\sim$ class B.

If the insulin-enhancing complex is slightly stable, like for class C ligands, it cannot compete with transferrin and albumin for the $V^{IV}O^{2+}$ complexation and, independently on the geometry in water, vanadium is mainly transported as (VO)hTf and (VO)$_2$hTf (Scheme 3). As demonstrated recently,[32] a small amount of $V^{IV}O^{2+}$ will

Scheme 3. Possible Biotransformations of an Insulin-Enhancing Compound Formed by Class A, B, and C Ligands in Blood Serum[a]

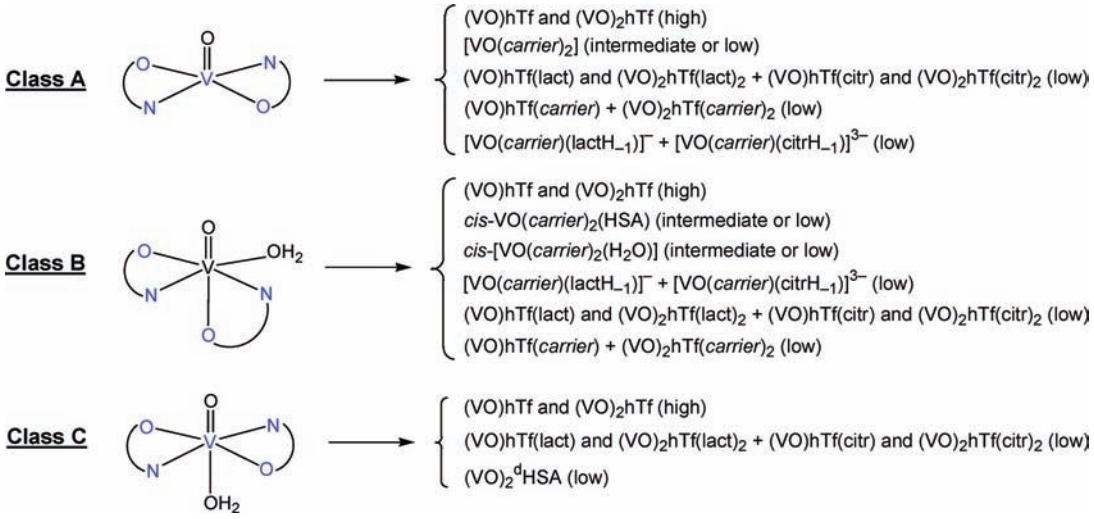

[a] For each class, between round brackets the concentration expected is indicated.

be present as ternary species with lactate and citrate, (VO)hTf(lact), $(VO)_2$hTf$(lact)_2$, (VO)hTf(citr), and $(VO)_2$-hTf$(citr)_2$, in which lactate and citrate behave as a synergistic anion[75] replacing bicarbonate in the specific sites of iron,[76] and as binary complex with albumin, $(VO)_2{}^{d}$HSA, where d indicates the dinuclear center with the two metal ions magnetically interacting.[77]

If the stability of the complexes increases, like for class A and B ligands, the percent amount of vanadium bound to transferrin as (VO)hTf and $(VO)_2$hTf will be lower, and the insulin-enhancing compound in its original form [VO(*carrier*)$_2$] and *cis*-[VO(*carrier*)$_2$(H_2O)] can survive (Scheme 3). Moreover, the organic *carrier* can interact with $V^{IV}O^{2+}$ ion as ternary complex with lactate and citrate, [VO(*carrier*)(lactH_{-1})]$^-$ and [VO(*carrier*)-(citrH_{-1})]$^{3-}$,[51] and forming species with stoichiometry (VO)hTf(*carrier*) and $(VO)_2$hTf(*carrier*)$_2$ in which it acts as synergistic anion (in its turn connected with the presence of one carboxylate group in the structure):[75] this has been recently demonstrated for picolinate.[78] If the geometry of insulin-enhancing compound in aqueous solution is *cis*-octahedral, like for class B ligands, mixed complexes with albumin can be formed, in which HSA replaces the water molecule in one of the four equatorial positions with an imidazole nitrogen of a histidine residue (*cis*-VO(*carrier*)$_2$(HSA)).[32,78] This is expected also for potent insulin-enhancing agents formed by 2,5-dipicolinic acid and its monoesters (class B),[27,28] but not for class A compounds that do not have a free equatorial position; as an example, it has been found that [VO(acetylacetonato)$_2$], that like class A ligands stabilizes square pyramidal geometry, does not yield mixed species with albumin.[32]

The possible transformation of an insulin-enhancing compound formed by class A, B, and C ligands in blood serum are shown in Scheme 3. The concentration expected (high, intermediate or low) is indicated for each species between round brackets. It must be, however, remembered that such a biotransformation depends not only on the thermodynamic factors but also on the kinetic behavior of the complexes.

Conclusions and Outlook

On the basis of the potentiometric, spectroscopic and DFT results, the picolinate and quinolinate derivatives have been divided into the classes A, B, and C.

The ligands belonging to class A in aqueous solution form bis chelated complexes (VOL_2) with *trans* arrangement of the donor atoms and in the solid state precipitate in square pyramidal geometry without water molecules coordinated to the metal ion. This behavior is expected for the ligands with a substituent in the *ortho* position to the carboxylic group, like 3-methylpicolinic and 1-isoquinolinecarboxylic acid, and for those forming six-membered chelate rings, like 2-pyridylacetic acid; the preference for the ligands that close chelate cycles with six terms to yield square pyramidal, pentacoordinated structures has been highlighted in the literature.[57c] The complexes formed by class A ligands follow a normal EPR behavior.

Class B comprises the ligands that form bis chelated species (*cis*-$VOL_2(H_2O)$) with one of the two ligand molecules adopting an (equatorial-axial) arrangement and an equatorial water-O in *cis* position with respect to V=O bond; they give rise to a hydroxido, EPR-active species (*cis*-$VOL_2(OH)$) with an OH^- ion that replaces H_2O molecule in the equatorial site. In the solid state and after dissolution in coordinating and non-coordinating solvents, they retain the *cis* form observed in aqueous solution. Class B includes picolinic acid and its derivatives without substituents in *ortho* position to the carboxylic group or aromatic nitrogen (for example the ligands substituted in position 4 or 5, like 2,5-dipicolinic acid and its monoesters[27,28]). Such ligands are not sterically hindered, and the favorable solvation free energy favors the binding of a H_2O or OH^- ligand in the equatorial plane. As

(75) (a) Campbell, R. F.; Chasteen, N. D. *J. Biol. Chem.* **1977**, *252*, 5996–6001. (b) Sun, H.; Cox, M. C.; Li, H.; Sadler, P. J. *Struct. Bonding (Berlin)* **1997**, *88*, 71–102.

(76) Sanna, D.; Micera, G.; Garribba, E. *Inorg. Chem.* **2009**, *48*, 5747–5757.

(77) Sanna, D.; Garribba, E.; Micera, G. *J. Inorg. Biochem.* **2009**, *103*, 648–655.

(78) Sanna, D.; Buglyó, P.; Micera, G.; Garribba, E. *J. Biol. Inorg. Chem.* **2010**, *15*, 825–839.

observed for the species formed by class A ligands, they respect the "additivity rule".[53−55]

Class C ligands form bis chelated species that in aqueous solution undergo an equilibrium between the square pyramidal and *trans*-octahedral form, VOL_2 and *trans*-$VOL_2(H_2O)$. Such ligands have a peculiar structure with an alkyl in *ortho* position to the pyridine nitrogen (6-methyl or 6-ethylpicolinic acid) or an aromatic ring condensed with that of picoline to give a quinoline acid (quinaldic and kynurenic acid). In the solid state they precipitate with the two ligand molecules in the equatorial sites and with or without a water molecule coordinated in the axial position. In the last case, the geometry is strongly distorted toward the trigonal bipyramid, and four bands in the electronic absorption spectrum are expected.[65] After dissolution in DMSO, they yield both the penta- and hexa-coordinated species, whereas in a mixture CH_2Cl_2/toluene 50:50 v/v and in DMF only the square pyramidal and *trans*-octahedral species, respectively, are formed. The *trans*-octahedral compound is characterized by an anomalous EPR response, with A_z lower by about 10% than the value calculated on the basis of the "additivity rule".[59] When in the solid state the species is penta-coordinated, like $[VO(6\text{-mepic})_2]$, the frequency stretching of V=O bond can be reduced by the axial interaction between the oxido-O with the free coordination site of another molecule.

These features were confirmed by a search from the Cambridge Structural Database[79] for monomeric $V^{IV}O^{2+}$ compounds with bidentate ligands provided with (N, O) donor set, that yielded 34 structures; among them, 29 precipitate without water/solvent coordinated to the metal ion and exhibit a square pyramidal geometry. Only five complexes have a water molecule bound to $V^{IV}O^{2+}$: two are formed by class C ligands, 6-ethylpicolinic and quinaldic acid, *trans*-$[VO(6\text{-etpic})_2(H_2O)]$[25] and *trans*-$[VO(quin)_2(H_2O)]$;[63] two are formed by derivatives of picolinic acid (class B), *cis*-$[VO(5MeOpic)_2(H_2O)]$[27] and *cis*-$[VO(5\text{-}i\text{PrOdipic})_2(H_2O)]$;[28] the fifth structure, *cis*-$[VO(HDMCI)_2(H_2O)]$,[58] is very similar to these latter, with the H_2O ligand in the equatorial plane and a carboxylate-O in the axial position. Therefore, H_2MDCI can be considered a class B ligand. On the whole, these hits confirm the tendency of the complexes formed by class B and C ligands to bind a water molecule in the first coordination sphere, forming a hexa-coordinated structure with *cis*- or *trans*-octahedral geometry. However, it must be highlighted that several factors can contribute to determine the final stoichiometry and the geometry of the compound, such as the electronic and steric requirements of the ligand and, mainly, the solvation effects.

(79) Allen, F. H.; Kennard, O. *Chem. Des. Autom. News* **1993**, *8*, 31–37.